UNIVERSITÀ DEGLI STUDI DI VERONA

DIPARTIMENTO DI MEDICINA

SEZIONE DI PATOLOGIA GENERALE

Scuola di dottorato di Scienze della Vita e della Salute

Dottorato di Ricerca in Infiammazione, Immunità e Cancro

Ciclo XXXV

NOVEL ISOFORMS OF THE GIANT PROTEIN TITIN IN THE REGULATION OF LYMPHOCYTE TRAFFICKING

S.S.D. MED/04 PATOLOGIA GENERALE

Coordinatore: Prof. Vincenzo Corbo

Supervisor: Prof. Carlo Laudanna

Co-supervisor: Dott.ssa Lara Toffali

Dottoranda: Dott.ssa Beatrice D'Ulivo

NOVEL ISOFORMS OF THE GIANT PROTEIN TITIN IN THE REGULATION OF LYMPHOCYTE TRAFFICKING
Tesi di dottorato
Verona, 13/03/2023

ABSTRACT

Titin (TTN) is the largest protein in the human genome and is mainly known as the third component of the sarcomere together with actin and myosin. In this context, TTN is responsible for maintaining muscle passive stiffness providing structural, scaffolding, and mechano-signaling properties. Here, we describe unexpected role of TTN in the regulation of human lymphocyte physiology. Human T lymphocytes express three novel TTN isoforms exhibiting cell-specific expression and different distribution to subcellular compartments. By performing fluorescence microscopy 3D imaging, we found that the LTTN1 and the LTTN2 isoforms span cytosolic as well as nuclear compartments, whereas the smallest LTTN3 isoform seems to be restricted to the cytosol. Recent data from our laboratory showed that LTTN1 covers a pivotal role in immune system physiology. Indeed, LTTN1 controls microvilli stricture and, thus, selectin-mediated tethering and rolling, chemokine-triggered integrin activation, chemotaxis, and *in vitro* cell deformability underflow. The new *in vivo* data confirmed LTTN1 putative role in T lymphocytes resilience to mechanical stress induced by passive deformation in the microcirculation. This makes LTTN1 a crucial player not only in multiple steps of T lymphocyte trafficking but, and importantly, in T lymphocyte survival. Besides LTTN1, we demonstrated that also LTTN3 is involved in the *inside-out* pathway of chemokine-triggered integrin activation. LTTN3 facilitates chemotaxis and controls chemokine-triggered integrin-mediated adhesion. Accordingly, it mediates RhoA and Rac1 small GTPases activation. Thus, while LTTN1 is a critical housekeeping regulator of T lymphocyte physiology, our results also suggest a possible involvement of LTTN3 as a central modulator of chemokine-induced signal transduction in T lymphocytes.

ABBREVIATIONS

AO *Acridine Orange*

ARVC *Arrhythmogenic Right Ventricular Cardiomyopathy*

CNM *Centronuclear Myopathy*

CRD *C-terminal Regulatory tail Domain*

CXCL *C-X-C Motif Chemokine Ligand*

CXCR *C-X-C Motif Chemokine Receptor*

DCM *Dilated Cardiomyopathy*

DRM *Detergent-Resistant Membrane domain*

EOMFC *Early-Onset Myopathy with Fatal Cardiomyopathy*

ERM *Ezrin Radixin Moesin*

FBS *Fetal Bovine Serum*

FNIII *Fibronectin Type-III Domains*

G-LISA *GTPase-Linked Immunosorbent Assay*

GEF *Guanosine Exchange Factor*

GPCR *G-Protein Coupled Receptor*

HCM *Hypertrophic Cardiomyopathy*

HMERF *Hereditary Myopathy with Early Respiratory Failure*

HRP *Horseradish Peroxidase*

ICAM-1 *Intercellular Adhesion Molecule 1*

JAK *Janus Kinase*

KD *Knock Down*

LFA-1 *Lymphocyte Function-associated Antigen 1*

LGMD *Limb-Girdle Muscular Dystrophy*

MAC-1 *Macrophage Antigen 1*

MADCAM-1 *Mucosal Vascular Addressin Cell Adhesion Molecule 1*

MmDHD *Multi-minicore Disease with Hearth Disease*

MS *Mass Spectrometry*

MURF *Muscle Ring Finger Protein*

MyBPC *Myosin-Binding Protein C*

NCBI *National Center for Biotechnology Information*

PBS *Phosphate Buffered Saline*

PCR *Polymerase Chain Reaction*

PIP5KC *Phosphatidylinositol-4-Phosphate 5-Kinase Type 1 γ*

PK *Protein Kinase*

PLD1 *Phospholipase D1*

PSGL-1 *P-Selectin Glycoprotein Ligand 1*

PTK *Protein Tyrosine Kinase*

RCM *Restrictive Cardiomyopathy*

RNA-Seq *RNA Sequencing*

RPMI *Roswell Park Memorial Institute Medium*

Scr *Scrambled*

siRNA *small interfering RNA*

TK *Titin Kinase*

TMD *Tardive Tibial Muscular Dystrophy*

TTN *Titin*

VCAM-1 *Vascular Cell Adhesion Molecule 1*

VLA-1 *Very Late Antigen 1*

VVO *Vesiculo-Vacuolar Organelle*

INTRODUCTION

1. Titin

Titin (TTN) is known as the largest protein encoded by the human genome. Indeed, its name arises from the word "Titans", a species of giants in Greek mythology [1]. Together with actin and myosin, it represents the third cytoskeletal filament in the sarcomere of both cardiac and skeletal muscle of vertebrates [2]. No giant molecule that is comparable to titin has been found to span half the sarcomere in invertebrate striated muscles. Instead, based on the abundance of Ig or fibronectin domains, titin-like proteins of various sizes in invertebrates have been identified and distinguished into two main classes: those that resemble the I-band part of titin in their domain composition, such as kettins and stretchins, and those that resemble the A-band part, like twitchins and projectins [3].

The gene encoding for Titin (*TTN*) is located on chromosome 2q31 and consists of 364 exons among which the first is non-coding and the following 363 are coding [1,4]. Although the alternative splicing of the *TTN* gene could theoretically generate more than one million splice variants, only thirteen are annotated in the National Center for Biotechnology Information (NCBI) database, and their molecular weight span from ~600 kDa to ~3,7 MDa [2,3]. Indeed, the splicing profile of the *TTN* transcript and how and which exons are transcribed, is still unclear and remains under investigation [4].

1.1. Titin in muscle

While actin and myosin filaments mainly contribute to active force generation in the context of the sarcomere, titin filaments determine sarcomeric viscoelasticity, contributing to muscle cell passive stiffness [5]. In this context, titin behaves as a spring and a ruler, ensuring sarcomere tension and length. Moreover, the large size and the modular structure of titin make it an ideal architectural protein that provides support and maintains the sarcomeric organization during contraction. Titin covers also a sensory and signaling role as it participates in mechano-chemical signaling events through its multiple binding partners [1].

The titin molecule extends from the sarcomeric Z-disk, where the N-terminal Z-line region of the protein is located, to the sarcomeric M-band, where the C-Terminal M-line region of titin overlaps in antiparallel orientation with another C-terminal TTN molecule. Overall, the protein is organized in four structural and functional areas, extending over a length of 1.2 µm. Indeed, between the Z- and the M-line, are found the elastic I-band and the thick A-band regions (Fig. 1). While the Z-line, the M-line, and the A-band regions are extremely conserved, the I-band sequence defines the different properties of each different TTN isoform [1,2,5].

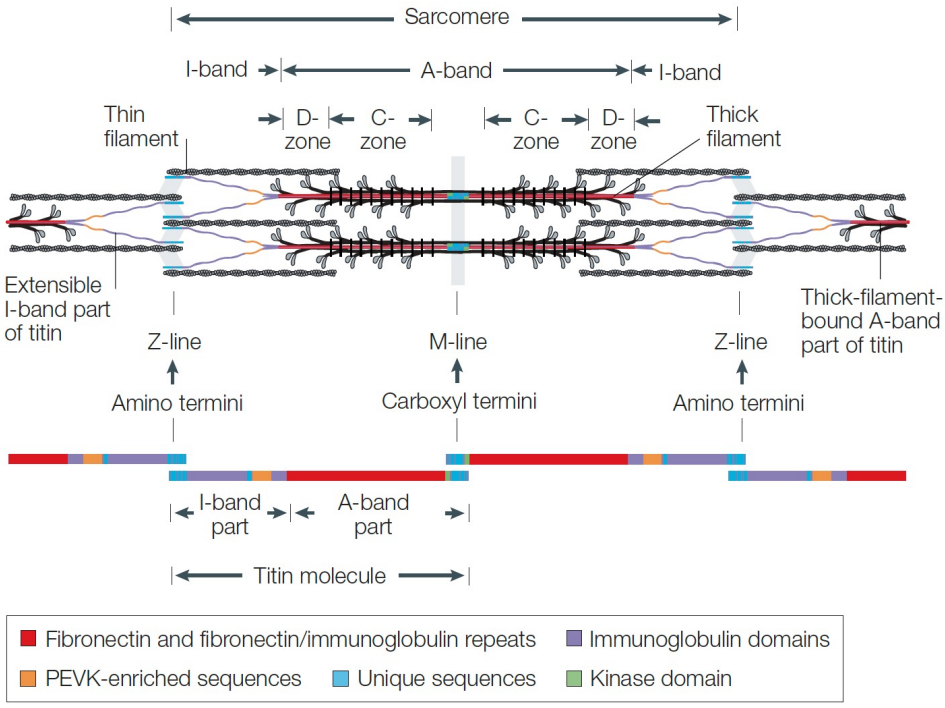

Fig. 1. The structure of vertebrate striated muscle sarcomere [3].

1.1.1. The Z-line

The Z-line embeds the N-terminal segment of TTN and acts as an anchor for the protein to the Z-disk of the sarcomere. This firm binding is likely obtained through the binding of the Z-repeats, a repeated motif of ~45 residues belonging to a differentially spliced unique sequence, to α-actinin, which crosslinks anti-parallel thin filaments from adjacent sarcomeres [2,3]. Depending on the type of striated muscle and the developmental stage, the copy number of the Z-repeats can vary

from 2 to 7. Besides the presence of Z-repeats, the Z-line of TTN contains multiple Ig-like domains and large interdomain sections that concurrently interact with different Z-line proteins. Among them, the two amino-terminal Ig domains present a binding site for telethonin (T-cap), a protein that is specifically expressed in cardiac and skeletal muscle and is involved in many cellular signaling mechanisms as well as sarcomere stability. In the junction between Z-line and I-band, the Ig motif bind to obscurin, tropomyosin, and the Ca^{2+}-dependent protease calpain-1 [2] (Fig. 2).

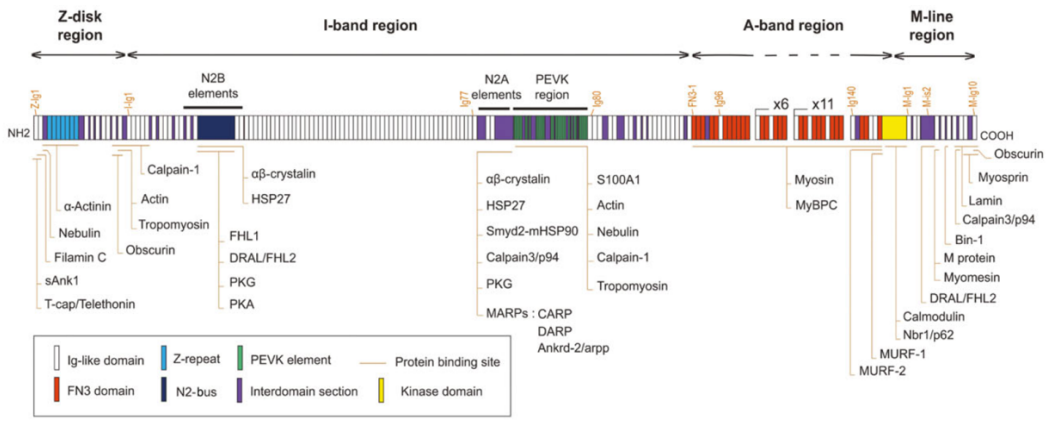

Fig. 2. Titin protein partners [2].

1.1.2. The I-band

The I-band represents titin extensible region and enables the protein to maintain its Z- and M-line connection during muscle elongation and contraction. As this region acts as a molecular spring, is not surprising that its differential splicing is responsible for the high variability of titin elastic properties among different isoforms [2,6]. Indeed, upon splicing of few Ig domains and PEVK repeats, the titin springs become shorter and so less compliant than those with more exons spliced in. Accordingly, shorter, and stiffer I-band parts belong to the isoforms present in stiffer muscles, such as cardiac muscles, while longer and more compliant I-band regions are found in extensible muscles, such as the skeletal soleus[3].

The I-band is composed of tandem Ig domains interspersed with unique sequences. The amino-terminal region of the I-band is composed of 15 Ig-like domains that are

conserved between isoforms. This “proximal” part is sequentially followed by the N2 region, which is composed of Ig domains and unique sequences; the unique PEVK region, mainly encompassing proline (P), glutamate(E), valine (V), and lysine (K) residues, that confers titin elastic properties; and the final carboxy-terminal I-band segment, which contains 22 Ig domains [2,3,6].

Depending on the tissue, there are two alternative forms of the N2 region; in skeletal muscle, titin contains the N2A sequence, whereas cardiac titin presents either N2B or both N2A and N2B sequences (also called N2BA titin isoform). Some cardiac isoforms also present additional areas of unique sequences called novex-1 and novex-2, while both cardiac and skeletal muscle could present a truncated titin small isoform called novex-3 (~700 kDa) which arises from the expression of a stop codon present on exon 48 [2,3,6]. The unique sequences present in the I-band region constitute hotspots for interactions with signaling molecules involved in protein quality control, phosphorylation, or oxidation pathways that lead to modification in titin-based passive stiffness. For example, specific protein kinases (PKs) such as PKA and PKG are known to phosphorylate the cardiac N2B leading to a decrease in titin stiffness. On the contrary, phosphorylation of PEVK elements by PKCα increases titin stiffness [2,6] (Fig. 2). The binding of calpain-1 and -3/p94 in the proximity of the PEVK elements and the N2 region suggests a role for titin also in protein turnover [2,6,7].

1.1.3. The A-band

The A-band harbors the largest part of TTN. Through interactions with myosin-binding protein C (MyBPC) and multiple interactions with myosin through the fibronectin type-III domains (FNIII) of titin, this region acts as a stabilizer for the assembly of the thick filament. The A-band sequence is highly conserved between muscle types and species and contains both Ig and FNIII domains that are arranged in two types of structures: a seven-domain segment repeated six times, adjacent to the I-band/A-band junction, and an eleven-domain stretch occurring eleven times [2,3,5]. At the end of the A-band are present binding sites for the members of E3-ubiquitin ligase muscle ring finger protein (MURF)-1 and -2 (Fig. 2), which are known to be multifunctional adaptor proteins that may have a role in gene

expression regulation pathways and in protein turnover acting as ubiquitin ligase [2,5].

1.1.4. The M-line

The M-line directly connects adjacent tick filaments in the middle of the sarcomere. Indeed, proteins such as myomesin and M-protein, which directly interact with TTN, provide structural linkage between thick filaments [3].

The M-line region of titin contains the carboxyl terminus of the protein and is composed of 10 Ig domains interspersed with unique sequences. This portion harbors a unique serine-threonine kinase domain (TK) and several protein binding domains that make the M-line a hotspot for protein-protein interactions [3,5]. Among them, obscurin and calpain-3/p94 are known interaction partners for M-band titin [5]. During muscle stretch and contraction, the sarcomeric M-line is subjected to mechanical deformation that consequently brings muscle remodeling in response to the mechanical load applied as well as physiological stress [8,9]. Even if little is known about the mechanisms by which mechanical and physiological signals are integrated to result in a trophic response, the kinase domain of TTN seems to play a central mechanosensory function. Indeed, since TK presents undetectable levels of catalysis, is considered a pseudokinase that is likely to translate mechanical signals into regulatory pathways of gene expression and protein turnover in the myofibrils through a scaffolding activity [8–10]. These mechanosensing properties of titin kinase seem to be mediated by stretch-induced conformational changes in the protein during muscle function. Notably, the C-terminal regulatory tail extension (CRD) that sterically inhibits the TK active site, is reversibly unfolded upon stretch allowing the exposure of cryptic binding sites on the protein. In its active conformation, TK is reported to bind the autophagy receptors Nbr1, p62, and MURF-1 and -2 ubiquitin ligases (Fig. 2), thus linking mechanosensing to the trophic response of the myofibril [8,9,11].

1.2. Titin in diseases

Considering the huge size and the multiple functions, mutations targeting titin can have different biological effects and result in cardiac or skeletal muscle myopathies. There are over one hundred disease-associated mutations reported titin in literature for human titin. Some annotated *TTN* gene mutations lead to a purely skeletal muscle phenotype, while the majority have been associated with a purely cardiac phenotype. However, few mutations affect both cardiac and skeletal muscle tissues [2]. The genotype-phenotype correlation of most titin mutations remains still under investigation. Indeed, relatively few patients have undergone a full *TTN* gene screen and the experimental challenges encountered to study this huge protein as well as functionally validate its variants make their pathogenic impact still unclear [1,2]. Here are reported some of the diseases associated with *TTN* mutations.

a) Purely skeletal muscle disorders with no cardiac involvement

- *Tardive tibial muscular dystrophy (TMD)*

  TMD is an autosomal dominant, late-onset distal myopathy characterized by muscle weakness and atrophy of the anterior compartment of the lower leg muscle, in particular the tibialis anterior muscle. Clinical symptoms usually occur after the age of 35. The mutations causing TMD map to the M-line of TTN and can be caused by a series of genetic alterations including deletions or indel variations, missense, or nonsense mutations [2,12].

- *Limb-girdle muscular dystrophy (LGMD)*

  LGMD is a genetically heterogeneous disorder caused by mutations in many different genes encoding proteins that are implicated in muscle maintenance and repair [12,13]. Inheritance can be either autosomal dominant or autosomal recessive and based on it, LGMDs are classified as Type 1 and Type 2 respectively. The titin-related disease is named limb-girdle muscular dystrophy type 2J and is caused by mutations that alter the C-terminal calpain3/p94-binding domain of the protein. Concerning the clinical manifestations, the disease is characterized by progressive wasting and weakness of the proximal muscles of arms and legs, particularly in the pelvic or shoulder girdles [2,13].

- *Hereditary myopathy with early respiratory failure (HMERF)*

HMERF is an autosomal dominant disease characterized by adult-onset. Patients affected by this disorder present weakness in proximal and distal parts of the upper and lower extremities and respiratory muscles, particularly the diaphragm [2]. *TTN* gene mutations are associated with HMERF and target both the A-band region and the kinase domain of titin. Considering its central role in regulating the assembly and the length of the thick filaments, and the presence of several sites of interactions with ligands, mutations in the A-band region are likely to cause sarcomere disruption [14]. Furthermore, the exchange of a conserved arginine to tryptophan in the TK regulatory tail has been shown to disrupt the Nbr1/p62/MURF2 pathway, thereby perturbating the link between mechanosensing and the trophic response of the myofibril [11].

- *Centronuclear myopathy (CNM)*

  CNM is a genetically heterogeneous disease characterized by skeletal muscle weakness and wasting, and typical child-onset. The name of this myopathy arises from the displacement of the nuclei in muscle cells. Indeed, they are localized in the center of the muscle fiber instead of their classical peripheral position. Mutations in the myotubularin (*MTM1*), dynamin 2 (*DNM2*), and amphiphysin 2 (*BIN1*) genes, which encode for proteins linked to T-tubule biogenesis and triad formation, have been associated with the X-linked, autosomal dominant, or autosomal recessive form respectively [15,16]. However, it has been reported that at least 12 autosomal-recessive mutations of the *TTN* gene are associated with CNM onset. Variations of skeletal muscle titin are supposed to cause the disassembly of the I- and A-band regions in the muscle fiber with centrally localized nuclei, with consequent failure in sarcomere structure maintenance and assembly [2,17].

b) Purely cardiac muscle disorders associated with TTN mutations

- *Dilated cardiomyopathy (DCM)*

  DCM is the most common form of cardiomyopathy. The disease is classified as familial (up to 30% of total cases) or sporadic and is characterized by ventricular dilatation and impaired heart contraction and

inotropy [2]. About 25% of familial and ~18% of sporadic cases are caused by mutations in the *TTN* gene leading to truncating variants of TTN [18]. However, the complexity and the huge size of TTN as well as the lack of myocardial tissue from patients, make it challenging to study the precise genotype-phenotype correlation of DCM pathology. Indeed, little is known about the real impact of each TTN variant in such disease [19]. The reported *TTN* gene mutations associated with DCM include nonsense changes, frameshift and missense mutations, and changes in gene splicing. Most of them affect the A-band region, while a few targeting the I-band, Z-disk, and M-band region have also been reported [2,5].

- *Arrhythmogenic right ventricular cardiomyopathy (ARVC)*

  ARVC is an autosomal dominant inherited myocardial disease characterized by fibrofatty replacement of the myocardium, mainly of the right ventricle, and susceptibility to arrhythmias that lead to heart failure. Mutations in genes encoding proteins implicated in cell-cell junctions at the intercalated disks are known to be involved in the pathogenesis of the disease. However, it has been shown that even TTN mutations are associated with ARVC pathology [1,2,20]. Among them, a mutation targeting the Ig-like domain 10 of the I-band region of titin, is likely to reduce the structural stability of the protein and consequently increase its susceptibility to proteolytic degradation. Considering the fundamental role of titin in multiple processes such as sarcomere assembly, protein turnover, scaffolding, and mechanosensing, the instability of the protein and the proteolytic degradation could lead to ARVC pathology through multiple pathways that are still under investigation [20].

- *Hypertrophic cardiomyopathy (HCM)*

  HCM is the most common cause of sudden death in young adults. It is characterized by thickening of the left ventricular wall, cardiomyocyte hypertrophy, contractile dysfunction, and potentially fatal arrhythmias. Disease etiologies have not been fully understood yet, but in most cases, it has an autosomal dominant trait. The majority of HCM cases are caused by mutations in genes encoding for sarcomeric proteins, but gain-of-function

mutations of the *TTN* gene have also been implicated in the pathology outcome [1,2].

- *Restrictive cardiomyopathy (RCM)*

  RCM is a very rare form of cardiomyopathy characterized by marked atrial enlargement, normal systolic function, and reduced diastolic volume of one or both ventricles. The progressive biventricular heart failure makes the overall prognosis of RCM poor [21]. The disease can be secondary to idiopathic or system disease, but most cases are likely to be genetically determined. The pattern of inheritance can be either x-linked, autosomal dominant, or autosomal recessive and most mutations in sarcomeric proteins that also cause HCM, are the cause of RCM. Recently a *TTN* missense variant affecting a conserved residue in an Fn3 domain at the junction of I- and A-band has been implicated in the pathogenesis of RCM, suggesting titin as a new protein implicated in the pathogenesis of this disease [2,21].

c) Combined cardiac and skeletal muscle disease associated with TTN mutations

- *Salih myopathy or early-onset myopathy with fatal cardiomyopathy (EOMFC)*

  EOMFC is an early-onset multi-minicore myopathy with heart disease which represents the first titinopathy involving both skeletal and cardiac muscle. Particularly, affected patients present from the early infancy delayed motor development with generalized muscle weakness, joint and neck contractures, and rigid spine. The dilated cardiomyopathy manifests later and usually leads to death due to heart rhythm disturbances [22]. The mutations identified in the *TTN* gene are deletions of the first three encoding exons of the M-line which cause frameshifts downstream the kinase domain and titin truncation [22,23]. The truncated proteins normally integrate into the sarcomere of both skeletal and cardiac muscles of EOMFC patients causing sarcomere disassembly and M-line disruption. Moreover, the truncated variants lack the calpain3/p94-binding site and caused a calpain3/p94 depletion in the skeletal muscle, demonstrating that protein truncation influences the amount of this skeletal muscle-specific protease [23].

Now Salih myopathy is included in the group of multi-minicore diseases with heart disease (MmDHD) that include all the clinically heterogeneous congenital diseases with skeletal muscle and heart involvement associated with *TTN* mutations [24].

2. Leukocyte trafficking

Leukocytes have the capability to migrate from the blood into the tissues to induce an efficient immune response. In the blood they are mainly inactive, quiescent, cells ready to get engaged and activated upon exposure to environmental factors derived from the tissues and presented on the luminal side of the blood vessel by endothelial cells. Upon rapid engagement, leukocytes are directed to extravasation into the site of infection or tissue injury [25].

Leukocyte recruitment, and all the subsequent steps of leukocyte trafficking, are complex processes controlled by multi-step cascades of adhesive interactions and activating signals as well as molecular and mechanochemical events. The entire process is divided into different phases: capturing, rolling, activation, arrest, stabilized adhesion, crawling, and transmigration (paracellular or transcellular) (Fig. 3) [25,26].

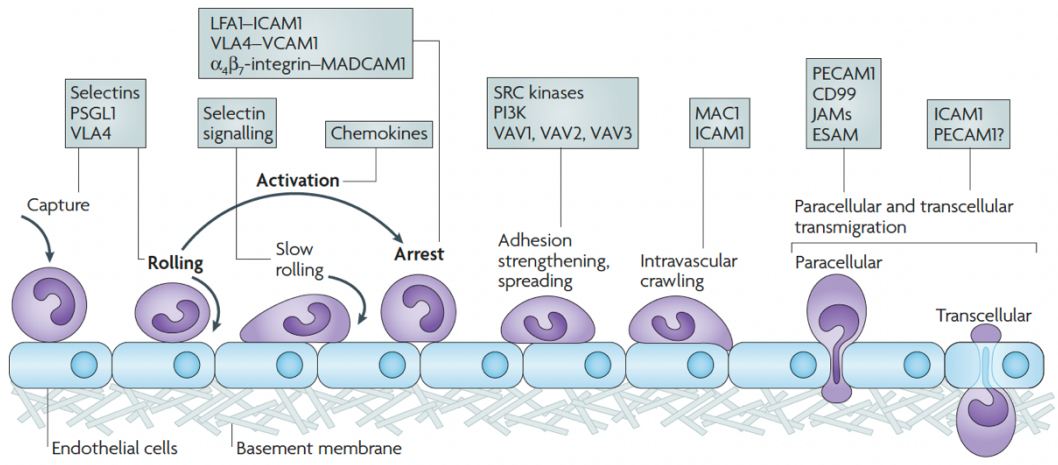

Fig. 3. Leukocyte adhesion cascade. Within the leukocyte adhesion cascade, each step is conditional to the next and mediated by key molecules indicated in the boxes [25].

2.1. Capturing and rolling

The initial tethering and rolling phases of the multi-step adhesion cascade are mainly mediated by the interaction of selectins with their ligands. The inflamed endothelium expresses E- and P-selectin (also expressed by platelets), while L-selectin is present on most leukocytes, clustered at the tips of microvilli [25,27]. The interaction of all these molecules with P-selectin glycoprotein ligand 1 (PSGL-1), expressed on almost all leukocytes, mediates capturing and rolling. The shear-stress exerted by the flowing blood is required to support the selectin-ligand interaction since the catch bond character of selectins allows the molecular bond to become stronger when a pulling force is applied to it. Indeed, the rolling cell detaches when the flow is stopped [25].

Rolling is frequently stabilized by leukocyte microvilli flattening, which slows down the rolling leukocyte and increases the topographical accessibility of both the chemokine receptors and integrins for interactions with their respective endothelial ligands [28]. Moreover, these slow rolling interactions enhance the efficiency of leukocyte interactions with chemoattractants expressed by endothelial cells and thus, the subsequent activation and arrest of the leukocyte itself. Indeed, the interaction of selectins with their ligands and the chemoattractant-mediated activation of G-protein coupled receptors (GPCRs), bring to the activation of strong stimulatory signals crucial for the following step of leukocyte arrest. Furthermore, also integrins may participate in rolling [25,28].

2.2. Activation, arrest, and adhesion

Concurrently to selectin-mediated rolling, and in response to chemoattractant stimulation, leukocyte integrins mediate the arrest on their endothelial ligands. These latter are represented by the endothelial immunoglobulin superfamily members, such as the vascular cell-adhesion molecule 1 (VCAM-1), the intercellular adhesion molecule 1 (ICAM-1), and the mucosal vascular addressin cell-adhesion molecule 1 (MADCAM-1). On the other hand, leukocyte integrins are cytoskeletally regulated transmembrane $\alpha\beta$ heterodimeric adhesive receptors such as the very late antigen 4 (VLA-4 or $\alpha_4\beta_1$-integrin; CD49d/CD29), the

lymphocyte function-associated antigen 1 (LFA-1 or $\alpha_L\beta_2$-integrin; Cd11a/CD18), and the macrophage antigen 1 (MAC1 or $\alpha_M\beta_2$-integrin; CD11b/CD18). VLA-4, LFA-1, and MAC1 bind to VCAM-1, ICAM-1, and MADCAM-1 respectively.

All circulating leukocytes maintain their integrins in mostly inactive states. However, integrins must undergo *in situ* activation and develop high affinity and valency for their ligands to establish shear-resistant firm adhesion on the target endothelial site [25,28]. Chemoattractants and chemokines such as CXCL12, CXCL8, CCL21, and many others, are the most potent physiologic integrin activators. After binding to specific GPCRs, chemokines, within few milliseconds, trigger complex intracellular signaling, known as *inside-out signaling*, that results in rapid integrin activation and increased avidity for the pro-adhesive surface. Concurrently, the interaction of integrins with their corresponding ligands transmits signals into the cell and generates the so-called *outside-in signaling*, allowing the cell to promptly respond to the signals sensed in the extracellular environment, thus mediating cell spreading, retraction, proliferation, and survival, along with adhesion stabilization and cell migration [25,29].

The modalities in which integrins undergo activation are at least two and they are identified as conformational changes, leading to increased affinity, and lateral mobility, leading to increased valency. They act as concurrent mechanisms to enhance cell avidity to the ligand (Fig. 4A) [26].

Whereas increased integrin affinity is caused by conformational changes of integrins that lead to an increase in the ligand-binding energy (and thus to a marked decrease in the rate of ligand dissociation), changes in valency involve integrin diffusion and clustering in the plasma membrane and corresponds to the density of integrin heterodimers per area of plasma membrane involved in cell adhesion [25]. Integrins first form small aggregates, called microclusters, all around the plasma membrane, and then they might redistribute on one side of the cell to create large patch-like clusters [29]. This disposition besides increasing valency also facilitates ligand engagement and the outside-in signaling events aimed at stabilizing cell arrest. Furthermore, to reach their functional conformation and increase the affinity for the ligand, integrins undergo dramatic structural changes that lead to the exposure of their ligand binding site [25,26].

LFA-1 is the most studied integrin in the context of integrin activation mechanisms. Its structure changes from a bent low-affinity conformation to an extended-intermediate- to a high-affinity conformation, which is defined by a complete opening of the ligand-binding pocket (Fig. 4B) [25,26,29]. However, LFA-1 extended conformations with great topographical availability of the ligand-binding headpiece can even present low affinity for the ligand. This conformation is likely to be involved both in chemokine-triggered arrest underflow and in increasing the capability of LFA-1 to mediate rolling on ICAM-1 upon selectin triggering [26].

The complex intracellular signaling cascade that regulates integrin activation is still under investigation. Several chemokine-induced signaling events have been linked to the regulation of integrin activation, but it appears that most of these pathways are limited to specific cell types and subsets of integrins, thus providing a complex layer of specificity [30,31].

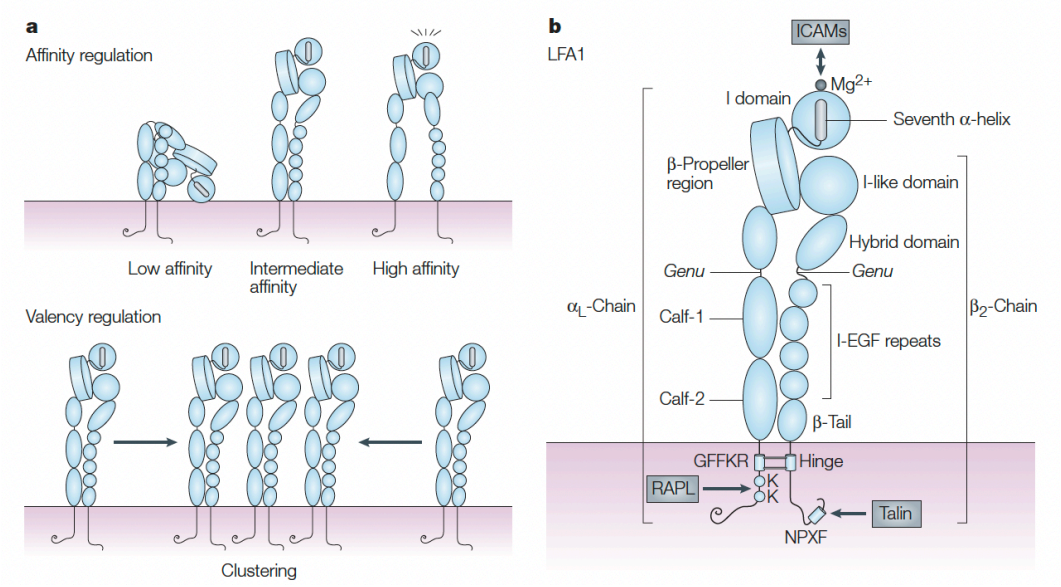

Fig. 4. Integrin structure and regulation. **A**, model of affinity (top) and valency regulation (bottom); **B**, structural representation of LFA-1 at high-affinity state [29].

It has been recently shown that chemokine receptor CXCR4 upon CXCL12 engagement triggers the activation of two independent, yet concurrent, pathways mediated by the Janus kinase (JAK) family of protein tyrosine kinases (PTKs), and the heterotrimeric $G\alpha_i$ protein. Together, they lead to the activation of multiple Guanidine Nucleotide Exchange Factors (GEFs), which in turn regulate small

GTPases activity. Rho and Rap modules are the validated GTPases involved in LFA-1 affinity triggering in human primary B and T lymphocytes. Together the two modules, through intermediate effectors such as phospholipase D1 (PLD1) and phosphatidylinositol-4-phosphate 5-kinase isoform-1γ (PIP5KC), regulate the activity of several actin proteins, such as FERMT3 and talin1, which, by interacting with integrin cytoplasmatic tail, lead the integrin conformational activation (Fig. 5) [29,31,32]. Moreover, it has been shown that both the Rho and Rap modules, besides leading to integrin conformational changes, also control integrin clustering at the plasma membrane, making them fundamental intermediators in both the two ways of integrin activation [30].

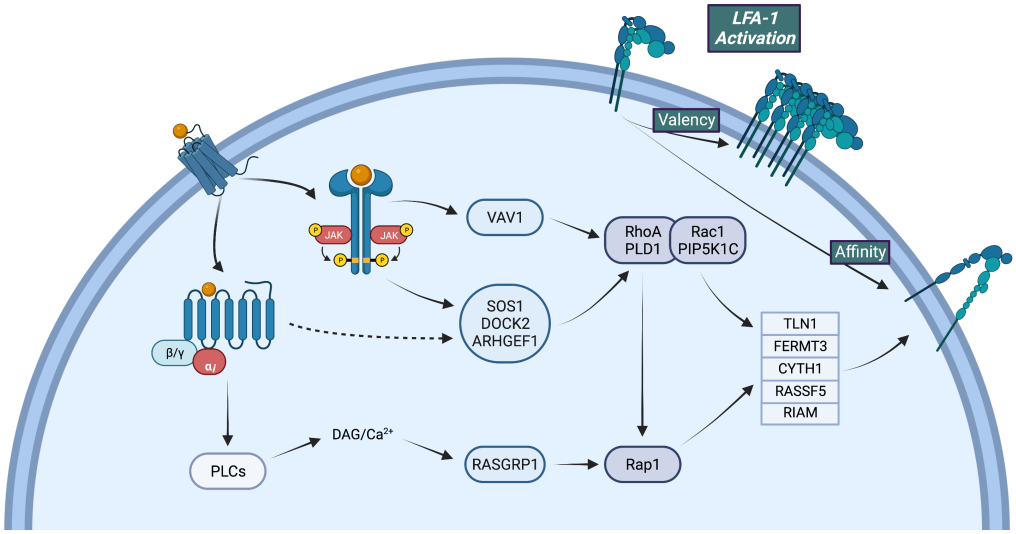

Fig. 5. Model of the inside-out signaling controlling LFA-1 affinity triggering by chemokines. CXCL12 binding to CXCR4 receptor induces the concurrent activation of JAK and $G\alpha_i$ protein, that in turn lead to the activation of multiple rho-GEFs. While VAV1 activity is JAK dependent, SOS1, DOCK2 and ARHGEF1 are regulated by both the kinase and the $G\alpha_i$ protein. The cooperation of these GEFs triggers RhoA and Rac1 GTPase activation. Rap1 activation is dependent on both RhoA and $G\alpha_i$ -dependent PLC regulation. Together, to regulate LFA-1-mediated rapid arrest, the Rho and Rap modules modulate the activity of several actin/integrin binding proteins. Modified from *Toffali L. et al.* [31].

2.3. Crawling and transmigration

Integrin clustering and allosteric conformational changes induced by the binding of integrin to the ligand, possibly contribute to the initiation of the signaling pathways

inside the cell that characterize the outside-in signaling. Altogether, these events lead to leukocyte spreading and migration, which occur upon a necessary cytoskeletal remodeling [25,33]. Indeed, chemokine stimulation of lymphocytes induces cell polarity by triggering the development of a leading edge (via actin polymerization) and the formation of a uropod at the rear, by actin-myosin-based contraction. Through a cyclic process of integrin-dependent attachment at the cell's front and detachment at the cell's back, the cell can crawl. Thus, leukocytes must integrate three kinds of stimuli to crawl productively on endothelial cells: inside-out signals generated upon the binding of a chemokine to the GPCR, outside-in integrin activation signals, and chemokine-triggered signals to actomyosin-remodeling mediated by Rho GTPases [34].

In lymphocytes, while both VLA-4 and LFA-1 can mediate cell arrest on activated endothelium, cell crawling under shear flow seems to be primarily mediated by LFA-1 [34]. Adherent lymphocytes, as well as other leukocytes, through the selectin-ligand binding, can induce the formation of endothelial-cell projections rich in ICAM-1 and VCAM-1. These cell-adhesion molecule microclusters are possibly triggered by the activation of a variety of endothelial GTPases (such as the Rho family) and may guide and initiate the transendothelial cell migration through transcellular or paracellular routes [25,34].

In the paracellular route, integrin ligation to the endothelial adhesion molecule reduces the inter-endothelial tight contacts, resulting in the passage of leukocytes through cell junctions. Indeed, upon the adhesion molecule binding to the integrin, endothelial cells increase the intracellular Ca^{2+} level, leading to the activation of p38 mitogen-activated protein kinase (MAPK) and Rho GTPase, that in turn induce cell contraction and junctions opening.

In the transcellular pathway, which occurs in the thin parts of the endothelium, leukocytes extend cell membrane protrusions into endothelial cells. ICAM-1 ligation induces ICAM-1 translocation to actin- and caveolae-rich regions inside the endothelial cell. Subsequently, the caveolae containing ICAM-1 connect to form vesiculo-vacuolar organelles (VVOs), that create an intracellular channel through which a leukocyte can move. Moreover, ezrin, radixin, and moesin (ERM) proteins might operate as linkers between ICAM-1 and cytoskeletal proteins such

as actin and vimentin, allowing their distribution all around the channel, thus providing structural support for the cell [25].

3. ERM proteins and microvilli stability

ERM (ezrin, radixin, and moesin) proteins are a family of widely distributed membrane-associated proteins which are crucial in maintaining and regulating the cortical actin organization cross-linking the cortical F-actin cytoskeleton to the plasma membrane [35,36]. They exist in two conformationally regulated forms: open (active) and closed (inactive). The association between the N-terminal FERM domain and the C-terminal tail masks membrane- and actin-binding sites in the closed form. However, molecular events such as phosphoinositide binding and phosphorylation, cause the activation of the ERMs leading to a decrease in the inhibitory self-interactions and unmasking actin- and membrane-binding sites. This allows the N-terminal domains to interact with membrane proteins, and the C-terminal domains to bind cortical actin [36–38]. ERM proteins have been implicated not only in cell shape determination, but also in membrane protein localization, transport, and signal transduction. Indeed, the attachment of membrane proteins to actin is required for several essential processes, including cell shape and surface structure determination, cell adhesion, motility, cytoplasmic division, phagocytosis, and the integration of membrane transport with signaling pathways. Thus, ERM family members represent a critical juncture in the integration of cortical functions. Microvilli are outer membrane finger-like protrusions supported by the actin cytoskeleton. As previously described, they are fundamental in the process of leukocyte trafficking, especially during the initial step of rolling. Indeed, the adhesion receptors promoting contact and rolling along endothelial cells, such as L-selectin and VLA-4, are selectively concentrated at the tips of microvilli [37,39]. Moreover, also chemokine receptors such as CXCR4 and CCR7 are clustered at the tips of microvilli [40,41]. This promotes a rapid receptor-ligand interaction and prompt activation of the intracellular signaling cascade that leads to leukocyte activation and adhesion. Thus, microvilli are likely to be signaling hubs for rapid encounter and transmission of GPCRs-mediated signals [40]. However, to allow strong adhesion

and subsequent migration of leukocytes across the endothelium, microvillus loss is necessary [37].

During the past decades, it has been extensively reported that ERM proteins play a crucial role in microvilli formation and stability [35–37,42]. Particularly, the phosphorylation of the ERM family members has been associated with the maintenance of microvilli, while it has been shown that their dephosphorylation (ezrin, T567; radixin, T564; moesin, T558) induced by chemokines results in the collapse of microvilli within a few seconds [37,42]. Recent findings propose Rac1 as the mediator of ERM proteins dephosphorylation. Indeed, in response to CXCL12, the small GTPase seems to be a central player in controlling the disassembly of microvilli and is likely to mediate this effect via the very rapid dephosphorylation-mediated inactivation of ERM proteins at least in human T lymphocytes [38]. Thus, the interplay between Rac1 and ERMs might be a critical node in the response of the cell to many stimuli that lead to cortical actin modulation.

Moreover, ERMs function as linkers of the TCR components to the actin filaments, ensuring the correct and necessary organization of the TCR machinery on microvilli for the initiation of the immune synapse. The gradual collapse of the microvilli promoted by ERM proteins dephosphorylation, and the subsequent remodeling of the actin cytoskeleton is likely to promote the formation of stable T cell-APC interactions. Thus, besides leukocyte adhesion on vascular endothelium and leukocyte polarization, the Rac1-mediated ERMs dephosphorylation could be a mechanism to reduce cell rigidity to facilitate also other processes such as the formation of the immune synapse [38,43].

AIM OF THE STUDY

Very recent data from our laboratory demonstrated the presence of the giant protein titin in T lymphocytes (Toffali L. *et al.*, manuscript in preparation).

Mass spectrometry (MS) analysis of detergent-resistant membrane domains (DRMs) isolated from human T lymphocytes, detected 16 peptides mapping to different TTN regions. RNA-Seq analysis and the subsequent PCR validation confirmed that human primary T lymphocytes express three novel titin isoforms, each encompassing distinct segments of the *TTN* cDNA consensus region. These isoforms were designated as LTTN1, LTTN2, and LTTN3. Since MS-detected peptides were assigned to LTTN1 and LTTN2, but not to LTTN3, possibly LTTN1 and LTTN2, but not LTTN3, are associated with DRMs.

LTTN1 has been demonstrated to be involved in controlling cell capturing underflow, signaling mechanisms of integrin activation by chemokines, and cell deformability. Here, we wanted to deeply understand the role of this isoform in human T lymphocyte physiology, based on our previous investigations. Particularly, we focused on studying the behavior of LTTN1-silenced T lymphocytes *in vivo* to validate the *in vitro* data demonstrating the involvement of LTTN1 in cell deformability. We also investigated the role of this isoform in microvilli collapse, looking for a possible interplay between LTTN1 and ERM proteins, known to be involved in microvilli stability. Furthermore, we wanted to understand the contribution of the other TTN isoform, LTTN3, to the physiology of T cells. Particularly, here we provide a comparison between LTTN1 and LTTN3 titin isoforms in controlling steps of T lymphocyte trafficking.

MATERIALS AND METHODS

1. Reagents

Human ICAM-1/Fc (Catalog N°. 720-IC), human VCAM-1/Fc (Catalog N°. 862-VC) and human CXCL12 (Catalog N°. 350-NS) were from R&D Systems (Minneapolis, MN, USA); fluorescein isothiocyanate (FITC) goat secondary antibody to mouse (Catalog N°. F2012) and phycoerythrin (PE) secondary antibody to rabbit (Catalog N°. P9537) were from Sigma-Aldrich (St. Louis, Missouri, USA); Alexa Fluor 488 goat anti-rabbit (Catalog N°. A11008) and Alexa Fluor 488 goat anti-mouse (Catalog N°. A11001) were from Invitrogen (Waltham, Massachusetts, USA); antibodies anti-LTTN1 T55 and T75, and antibody anti-LTTN2 A-Band were custom-made by Eurogentec (Liege, Belgium); antibody anti-LTTN3 TTN-Kin and A 168-170 were from Myomedix (Myomedix GmbH, Neckargemünd, Germany); IB4 mouse monoclonal antibody (anti-CD18) was from American Type Culture Collection (ATCC, Manassas, Virginia, USA); L-Selectin antibody (anti-CD62L, Catalog N°. 555544), anti-CD3 antibody (Catalog N°. 340440), Alpha4 antibody (anti-CD49d, Catalog N°. 555503), and PSGL-1 antibody (anti-CD162, Catalog N°. 556055) were from BD (Franklin Lakes, New Jersey, USA); CXCR4 antibody was from Biolegend (Catalog. N°. 306506, San Diego, CA, USA); Vybrant® DyeCycle™ Violet/SYTOX® AADvanced™ Apoptosis Kit was from Termo Fisher Scientific (Catalog N°. A35135, Waltham, Massachusetts, USA); KIM127 mouse monoclonal antibody was purchased from ATCC, 327A mouse monoclonal antibody was kindly provided by dr. Kristine Kikly (Eli Lilly and Co., Indianapolis, IN, USA); RhoA G-LISA activation assay Kit (Catalog N°. BK124) and Rac1 activation assay Kit (Catalog N°. BK128) were from Cytoskeleton (Denver, Colorado, USA); Rac1 monoclonal antibody (Catalog N°. MA5-37658) and RhoA recombinant rabbit monoclonal antibody (Catalog N°. MA5-32262) were from Invitrogen; siRNAs (ON-TARGETplus SMARTpool) for LTTN1 and LTTN3 were designed and chemically synthesized by Dharmacon (Lafayette, Colorado, USA) and provided as premixed pools; P3 Primary Cell 4D-Nucleofector X was from Lonza (Catalog N°. V4XP-3024, Basel, Switzerland, Europe); Anti-β-actin was from Sigma-Aldrich (Catalog N°. A2066); Bradford

reagent 5X was from Serva (Catalog N°. 39222.02, Catoosa, Oklahoma, USA); cOmplete, EDTA-free protease inhibitor cocktail was from Roche (Catalog N°. 11873580001, Mannheim, Germany); Immobilon Western Chemiluminescent HRP Substrate was from Merck Millipore (Catalog N°. WBKLS0500, Burlington, Massachusetts, USA); Mouse IgG HRP-linked secondary antibody (Catalog N°. NA931V) and Rabbit IgG HRP-linked secondary antibody (Catalog N°. NA934) were from Cytiva (Marlborough, Massachusetts, USA); Phospho-Ezrin (Thr567)/Radixin (Thr564)/Moesin (Thr558) (Catalog N°. 3141) antibody and Moesin (Q480) (Catalog N°. 3150) antibody were from Cell Signaling Technology (CST, Danvers, Massachusetts, USA); Acridine Orange (Catalog N°. A1301) and DAPI (Catalog N°. D1306) were from Invitrogen. CellTracker™ Orange CMTMR Dye, CellTracker™ Green CMFDA Dye, CellTracker™ Red CMTPX Dye and CellTracker™ Blue CMAC Dye were from Thermo Fisher Scientific; Ficoll Paque Plus (Catalog N°. 17144003) and Percoll (Catalog N°. 17089101) were from Cytiva; Bovine Serum Albumin (Catalog N°. A4503) and Triton X-100 (Catalog N°. T8787) were from Sigma-Aldrich; Fluoro Gel with DABCO™, Anti-Fading Mounting Medium was from Electron Microscopy Sciences (Catalog N°. 17985-02, EMS, Hatfield, Pennsylvania, USA); FSC 22 Clear Frozen Section Compound was from Leica Biosystems (Catalog N°. 3801480, Wetzlar, Germany, Europe).

2. Human primary T lymphocytes isolation

Human primary T lymphocytes were isolated from whole blood of healthy donors by Ficoll and Percoll gradients (Cytiva). The purity of T lymphocytes preparation was evaluated by flow cytometry after staining with anti-CD3 antibody (BD) and was more than 95%. University of Verona Ethics Committee approved experimentation involving human primary cells (authorization no. 5626/02-02-2012).

3. Immunofluorescence microscopy analysis of LTTN isoforms

3 x 10^6 T lymphocytes were fixed with formaldehyde 0.4% in PBS for 20 min at RT, washed with wash buffer (PBS + 5% FBS) by microcentrifugation at 3000

RPM for 3 min, and re-suspended in 100 µl of permeabilization buffer (PBS + 0.1% Triton X-100) for 7 min at 4°C. After washing as above, cells were incubated with blocking buffer (PBS + 5% FBS) for 15 min at 4°C, and then TTN specific primary antibodies were directly added and incubated for 40 min at 4°C. Cells were washed twice with blocking buffer and incubated for 40 min at 4°C with secondary antibody in blocking buffer. Finally, cells were stained with 1 µg/ml DAPI (Invitrogen) for 10 min in the dark, washed, transferred to glass slides, and mounted with Fluoro Gel with DABCO (EMS). Images were acquired with a wide field Zeiss AxioImager Z.2 deconvolution microscopy setting (Carlo Zeiss, Germany), equipped with Colibri 7 fluorescent LED illumination, motorized 3D scanning stage, and Hamamatsu ORCA-Flash4.0 V3 Digital CMOS camera, set at 8 bit output depth. 512x512 pixel ROIs were acquired with a 100x Plan Apochromatic oil immersion objective (AN 1.46). Each field was acquired with double fluorescent light illumination (385/30 nm ex. for DAPI and 475/36 nm ex. for Alexa Fluor 488). Automatic 3D image scanning was according to the Nyquist-Shannon sampling theorem, by using the inline ZEN 3.5 Nyquist Calculator. To achieve super resolution imaging, 3D sampling density was set at intervals of 100 nm, corresponding to about half of the calculated Nyquist sampling distance (oversampling). Oversampled 3D scans were, then, processed with Zeiss ZEN 3.5 by applying the advanced Zeiss Deconvolution (DCV) module. Image deconvolution was achieved by applying the Constrain Iterative algorithm, without auto-normalization to fully control the photon budget thus allowing full reassignment of photons from out of focus optical planes. Spectral linear unmixing was, finally, applied to remove overlapped spectral components and background noise. Deconvolved and unmixed 3D stacks were rendered and analyzed with the ZEN 3.5 Arivis 3D module. Image Ortho projections were generated with Zeiss ZEN 3.5.

4. LTTN1 and LTTN3 silencing by small interfering RNAs

Human T lymphocytes were plated at 5 x 10^6 cells/ml in RPMI, 2 mM glutamine, and 10% FBS for 2 h before silencing. Cells, suspended in nucleofector buffer at 10^7 cells/ml, were electroporated using the Amaxa 4D-Nucleofector (program EO-

115; P3 Primary Cell 4D-Nucleofector X) in presence of a pool of four scrambled (Scr) or four different specific LTTN siRNAs according to manufacturer's instructions. The efficiency of siRNAs nucleoporation was evaluated with fluorescein isothiocyanate-conjugated siRNAs; the efficacy of LTTN1 and LTTN3 silencing was systematically evaluated by cytofluorimetric analysis every 24 h for 5-6 days.

LTTN1 target sequences:

1) GUGGAGACAUUACAUAUUA
2) GGUACUCAAUCACUAAUUA
3) GAAUUGAUGUCCUGUGGAA
4) UGUGGAAGCUCGUCAUAUA

LTTN3 target sequences:

1) GAUAUAUUGUGGAGCGCAA
2) UGAAGAAUGUCCAACGUAA
3) GUGACUAGGUCCACGUUUA
4) GCGUAAAGGACAAGUGCUA

5. Cell viability

Human T lymphocytes were labelled for 20 min at 4°C with Vybrant® DyeCycle™ Violet/SYTOX® AADvanced™ Apoptosis Kit following manufacturer's instruction. Cell viability was analyzed by flow cytometry (MACSQuant Analyzer 10; Miltenyi Biotech).

6. Cytofluorimetric analysis of adhesion molecules and chemokine receptor expression

Human T lymphocytes were labelled for 30 min at 4°C with CD18-, CD49d- and CXCR4-specific antibodies. The expression level of the molecules was analyzed by flow cytometry (MACSQuant Analyzer 10; Miltenyi Biotech). Data are shown as Mean Fluorescence Intensity (MFI) normalized to isotypic control.

7. Cytofluorimetric analysis and western blot of cp-ERMs and moesin expression

Human T lymphocytes, differently treated and stimulated with 0.2 μM CXCL12 (R&D Systems), were fixed in formaldehyde 0.4% for 20 min at 4°C. Cells were washed and suspended in 100 μl of permeabilization buffer (PBS + 5% FBS + 0.5% saponin) containing Phospho-Ezrin (Thr567)/Radixin (Thr564)/Moesin (Thr558) and Moesin specific primary antibodies (CST), for 30 min at 4°C. After rapid wash, cells were suspended in 100 μl of permeabilization buffer containing specific secondary antibodies, for 30 min at 4°C. After washing, cells were suspended in ice-cold PBS and the expression level of the molecules was analyzed by flow cytometry (MACSQuant Analyzer 10; Miltenyi Biotech). Data are shown as Mean Fluorescence Intensity (MFI) normalized to isotypic control. For Western blot, cells, treated as above, were lysed in ice-cold 1% NP-40 buffer, containing phosphatase inhibitors and complete protease inhibitor cocktail. Lysates were quantified by Bradford assay (Serva), and equal amounts of proteins were subjected to 10% SDS-PAGE. Anti-Phospho-Ezrin (Thr567)/Radixin (Thr564)/Moesin (Thr558) and anti-Moesin antibodies were used to reveal cp-ERMs and Moesin. Anti-β-actin antibody (Sigma-Aldrich) was used as a loading control. Immunoreactive bands were visualized by ECL detection (Merck Millipore) after incubation with appropriate HRP-linked secondary antibody (Cytiva), and intensities of band signals were quantified by using ImageQuant LAS 4000 (GE Healthcare).

8. Static adhesion assay

Human T lymphocytes were suspended at 3 x 10^6 cells/ml in standard adhesion buffer. Adhesion assays were done on 12-well glass slides coated with human 1 μg/ml ICAM-1 or VCAM-1 in PBS; cells, suspended in 20 μl standard adhesion buffer, were added to the wells and stimulated for 120 s at 37°C with 5 μl of CXCL12 (R&D Systems), 200 nM final concentration. After rapid washing, adherent cells were fixed in ice-cold 1.5% glutaraldehyde in PBS and counted by computer-assisted enumeration using a dedicated macro in Fiji (ImageJ).

9. Measurement of LFA-1 affinity state

Human T lymphocytes suspended in standard adhesion buffer at 2 x 10^6 cells/ml were stimulated for 180 s with 0.05 µM CXCL12 (R&D Systems) under stirring at 37°C in the presence either of 327A antibody (reporter for extended conformation epitope related to a high-affinity state) or KIM127 (reporter for extended conformation epitope possibility corresponding to intermediate-affinity state) [33]. After rapid washing, the cells were stained with FITC-conjugated secondary antibody (Sigma-Aldrich) and analyzed by flow cytometry (MACSQuant Analyzer 10; Miltenyi Biotech).

10. RhoA and Rac1 activation

RhoA and Rac1 activations were determined using G-LISA activation assay kits, by adaption of the protocols as previously reported. Human T lymphocytes were stimulated or not with 200 nM CXCL12 (R&D Systems) for 120 s and were lysed for 15 min in the lysis buffer indicated in manufacturer's protocol. Protein concentrations were quantified by Precision Red (provided in the kit). Equal amounts of proteins were added in triplicate to a 96-well plate coated with the RhoA-binding domain of rhotekin or anti-Rac1-GTP protein and incubated at 4°C for 30 min. Wells containing only lysis buffer were used as blank samples. After washing, the amount of RhoA-GTP bound or Rac1-GTP bound to each well was revealed by an anti-RhoA Ab or anti-Rac1 Ab (provided in the kit), followed by a secondary HRP-labeled Ab and detection of HRP. Signals were measured with a microplate spectrophotometer (Victor™ X5 Multilabel Plate Reader, Perkin Elmer, Waltham, MA, USA) by quantifying absorbance at 490 nm.

11. Western blot of total RhoA and Rac1 expression

LTTN1-silenced human T lymphocytes were stimulated with 0.2 µM CXCL12 (R&D Systems) lysed in ice-cold 1% NP-40 buffer, containing complete protease inhibitor cocktail. Lysates were quantified by Bradford assay (Serva), and equal amounts of proteins were subjected to 12% SDS-PAGE. RhoA and Rac1 were revealed by immunoblotting with anti-RhoA and anti-Rac1 primary antibodies

(Invitrogen). Anti-β-actin antibody (Sigma-Aldrich) was used for loading control. After incubation with appropriate HRP-linked secondary antibody (Cytiva), immunoreactive bands were visualized by ECL detection (Merck Millipore), and intensities of band signals were quantified by using ImageQuant LAS 4000 (GE Healthcare).

12. Chemotaxis assay

Human T lymphocyte migration assays were performed using 3 μm transwell filters, inserted in 24-well plates. The bottom chamber was filled with 0.7 ml of RPMI + 10% FBS containing 10 nM CXCL12 (R&D Systems); the top chamber was filled with 0.15 x 10^6 cells in 0.2 ml of RPMI + 10% FBS. Plates were incubated for 120 min at 37°C. The inserts were, then, removed and the total number of cells migrated in the lower chamber was counted by flow cytometry (MACSQuant Analyzer 10; Miltenyi Biotech).

13. Permanence of LTTN1-silenced T lymphocytes in mouse pulmonary circulation

C57BL/6J mice (stock N°. 000664 |Black 6) were purchased from the Jackson Laboratory. Animals were housed in pathogen-free climate-controlled facilities (temperature 21±1°C and humidity 50±5%) and were provided with food and water ad libitum. Research involving animals was authorized by the Ethical Committee from the University of Verona and by the Italian Ministry of Health, Department of Veterinary Public Health, Nutrition and Food Safety, Directorate General of Animal Health and Veterinary Medicine (authorization no. 416/2020-PR), as required by Italian legislation (D. Lgs 26/2014) as for the application of European Directive (2010/63/UE). All efforts were made to minimize the number of animals used and their suffering during the experimental procedures. Human T lymphocytes, nucleoporated with a pool of four Scr (control) or four LTTN1-specific siRNAs, were alternatively labelled with CellTracker™ Orange CMTMR Dye or CellTracker™ Red CMTPX Dye (Thermo Fisher Scientific). 5 x 10^6 control and 5 x 10^6 silenced cells were mixed in a total volume of 200 μl of PBS + 5% FBS and co-injected in the tail vein of adult C57BL/6J female mice. After 30 min, the

animals were euthanized and, without perfusion, lungs were immediately collected and fixed in 4% paraformaldehyde for 24 hours; following, lungs were dehydrated in a sucrose 30% solution for 24 hours, embedded in FSC 22 Clear compound (Leica Biosystems), and finally frozen. 25 µm thick serial sections of different lung lobes were cut using Leica CM1520 cryostat. Sections were seeded on gelatin-coated glass slides, stained with DAPI (Invitrogen) as nuclear marker, and mounted with DABCO mounting medium. Images were acquired with a AxioImager Z.2 wide field deconvolution upright microscopy setting (Carlo Zeiss, Germany), equipped with Colibri 7 fluorescent LED illumination, motorized 3D scanning stage, and Hamamatsu ORCA-Flash4.0 V3 Digital CMOS camera, set at 16 output bit depth. 2048x2048 pixel images were acquired with a 10x Plan Apochromatic objective (NA 0.45), corresponding to 1.33x1.33 mm tissue area, encompassing a tissue volume of 0.045 mm^3. Each field was acquired with triple fluorescent light illumination to detect post-fixation DAPI nuclear staining of pulmonary tissue and vital staining with CMTMR or CMTPX of injected human T lymphocytes. Spectral linear unmixing was automatically applied to all images to remove overlapped spectral components and background auto-fluorescence. Green and red artificial colors were assigned to all images to evidence LTTN1-silenced and control cells, respectively. Unmixed images were analyzed with Zeiss Intellesis AI automatic segmentation and ZEN 3.5 Image analysis modules.

14. Cytofluorimetric analysis of LTTN1-silenced T lymphocytes in mouse circulation and lungs

Human T lymphocytes, nucleoporated with a pool of four Scr (control) or four LTTN1-specific siRNAs, were alternatively labelled with CellTracker™ Green CMFDA Dye or CellTracker™ Blue CMAC Dye (Thermo Fisher Scientific). 3 x 10^6 control and 3 x 10^6 LTTN1-silenced cells were mixed in a total volume of 200 µl of PBS + 5% FBS and co-injected in the tail vein of adult C57BL/6J female mice. After 30 min, the mouse was anesthetized, 450 µl of blood was collected from the orbital sinus, and erythrocytes were allowed to sediment using 0.5% dextran. The supernatant containing the injected T lymphocytes was analyzed by flow cytometry (MACSQuant Analyzer 10; Miltenyi Biotech). After blood collection, the lungs

were also collected, cut into small pieces with scissors and put in 2 ml of freshly prepared digest solution (1 mg/ml Collagenase and 0.5 mg/ml DNase). The sample was incubated at 37°C for 60 min in shaking to allow tissue digestion. Cells were washed, resuspended in FACS buffer, filtered through a 70 µm cell strainer and analyzed by flow cytometer (MACSQuant Analyzer 10; Miltenyi Biotech).

15. Intravital microscopy of LTTN1-silenced T lymphocytes in mouse muscle microcirculation

C57BL/6J mice were hosted as above and prepared according to previous studies [44–46]. Briefly, animals were anesthetized with an intraperitoneal injection of physiologic saline containing ketamine (5 mg/ml) and xylazine (1 mg/ml). For the injection of labelled cells, the right common carotid artery was cannulated with a heparinized PE-10 polyethylene catheter pointed toward the aortic arch. The skin was, then, reflected, and the pectoral muscle was bathed with saline; a coverslip (24x24 mm) was applied and fixed with silicon grease covering the pectoral muscle. Human T lymphocytes, nucleoporated with a pool of four Scr (control) or four LTTN1-specific siRNAs, were labelled with Acridine Orange (AO, Invitrogen) 0.1 mg/ml, washed twice in PBS, and directly injected in the right carotid with a digital pump (SP100; World Precision Instruments) at a flow rate of 1µl/s. The procedure allowed immediate arrival of labelled cells into muscle microcirculation, without previous passage in the great circulation, preventing entering other organs before imaging. Intravital imaging of striate muscle preparations was done with a AxioExaminer A1 microscope, equipped with Colibri 7 fluorescent LED illumination (Carl Zeiss, Germany). Imaging was at 5x magnification (AN 0.16) with fluorescence set at 492 nm_533/656 nm ex-em wavelengths. Digital movies were acquired with a Sony Alpha IV (ILCE-7M4) full frame (33 MP) camera allowing high resolution (4K), high framerate (50 fps) color video recording. Recorded MP4 movies were converted to AVI MJPEG and quantitative frame-by-frame analysis was done with Fiji. The image analysis field corresponded to a tissue area of about 2 mm^2. Four different behaviors of circulating cells were scored, including: a- cells that very rapidly crossed the field, with no interactions with the vascular wall; b- cells that very transiently (less than a sec.) interacted with the

vascular wall; c- cells that interacted with the vascular wall, eventually with a stop-and-go and/or entrapped behavior, but with no rear leakage of cell AO labeled content; d- cells that interacted with the vascular wall, eventually with a stop-and-go and/or entrapped behavior, but manifesting a progressive rear leakage of cell AO labeled content. Cells showing behavior “d” were scored as damaged cells and counted, along with all cells showing the other three different behaviors when crossing the imaging field. Data were expressed as % of cells manifesting behavior (d) over total cells crossing the imaging field.

RESULTS

1. LTTN1, LTTN2, and LTTN3 subcellular localization in T lymphocytes

Recent data from our laboratory demonstrated the presence of three novel TTN isoforms in T lymphocytes. Particularly, MS analysis of human T cells DRMs detected 16 peptides mapping to different TTN regions. Subsequent RNA-Seq analysis and PCR validation on T lymphocytes mRNA, confirmed the presence of three distinct TTN isoforms, each encompassing distinct segments of the *TTN* gene (Fig. 6). The newly discovered proteins were designated as LTTN1 (118 exons), LTTN2 (137 exons), and LTTN3 (15 exons). Predictive bioinformatic analysis showed that LTTN1 consists of 9382 amino acids with a MW of 1.04 MDa; LTTN2 consists of 19,044 amino acids with a MW of 2.11 MDa; LTTN3 consists of 3476 amino acids with a MW of 392 kDa and harbors the Serine-Threonine kinase domain. Since MS-detected peptides were assigned to LTTN1 and LTTN2, but not to LTTN3, possibly LTTN1 and LTTN2, but not LTTN3, are associated with DRMs. Domain reconstruction revealed the presence of multiple protein domains regulating protein-protein interactions, signal transduction, and the response to mechanical stress.

The expression of these three isoforms was also confirmed by flow cytometry with five different antibodies, each targeting a distinct region of TTN.

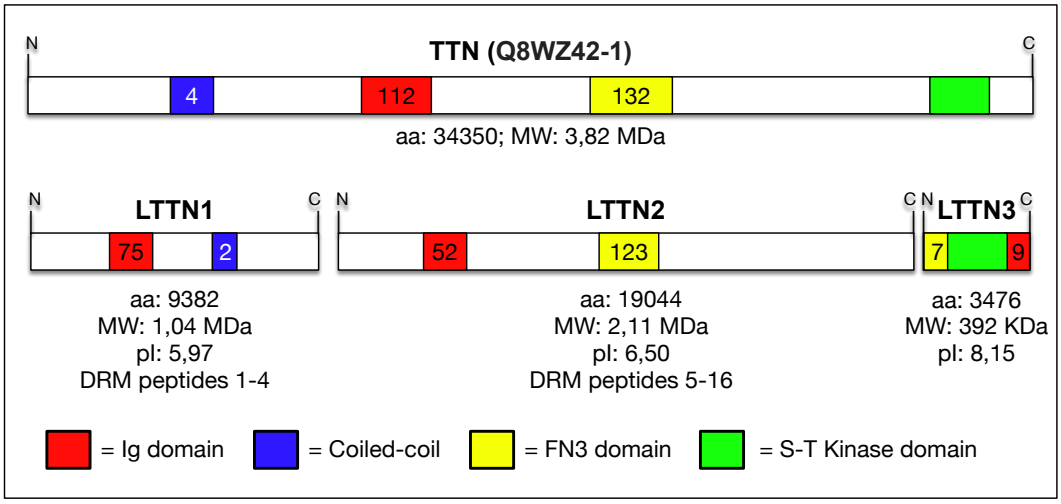

Fig. 6. The three novel TTN isoforms expressed in human primary T lymphocytes. Diagrams of novel TTN protein isoforms expressed in human T lymphocytes predicted from the transcripts reconstructed from RNA-Seq, compared to the canonical muscle isoform (UniProt ID Q8WZ42-1). The number of amino acids, MW, isoelectric point (pI) and the MS-identified peptides in DRMs are shown, along with the position and total number of immunoglobulin (red), coiled-coil (blue), fibronectin III (yellow) and S/T kinase (green) domains.

To explore the subcellular localization of LTTN1, LTTN2, and LTTN3, we exploited wide field fluorescence deconvolution microscopy, with photon budget readdressing to increase the detection sensitivity. 3D image analysis revealed distinct intracellular distribution for each isoform (Fig. 7), with LTTN3 confined to the cytosol whereas LTTN1 and LTTN2 localized to both cytosol and nucleus.

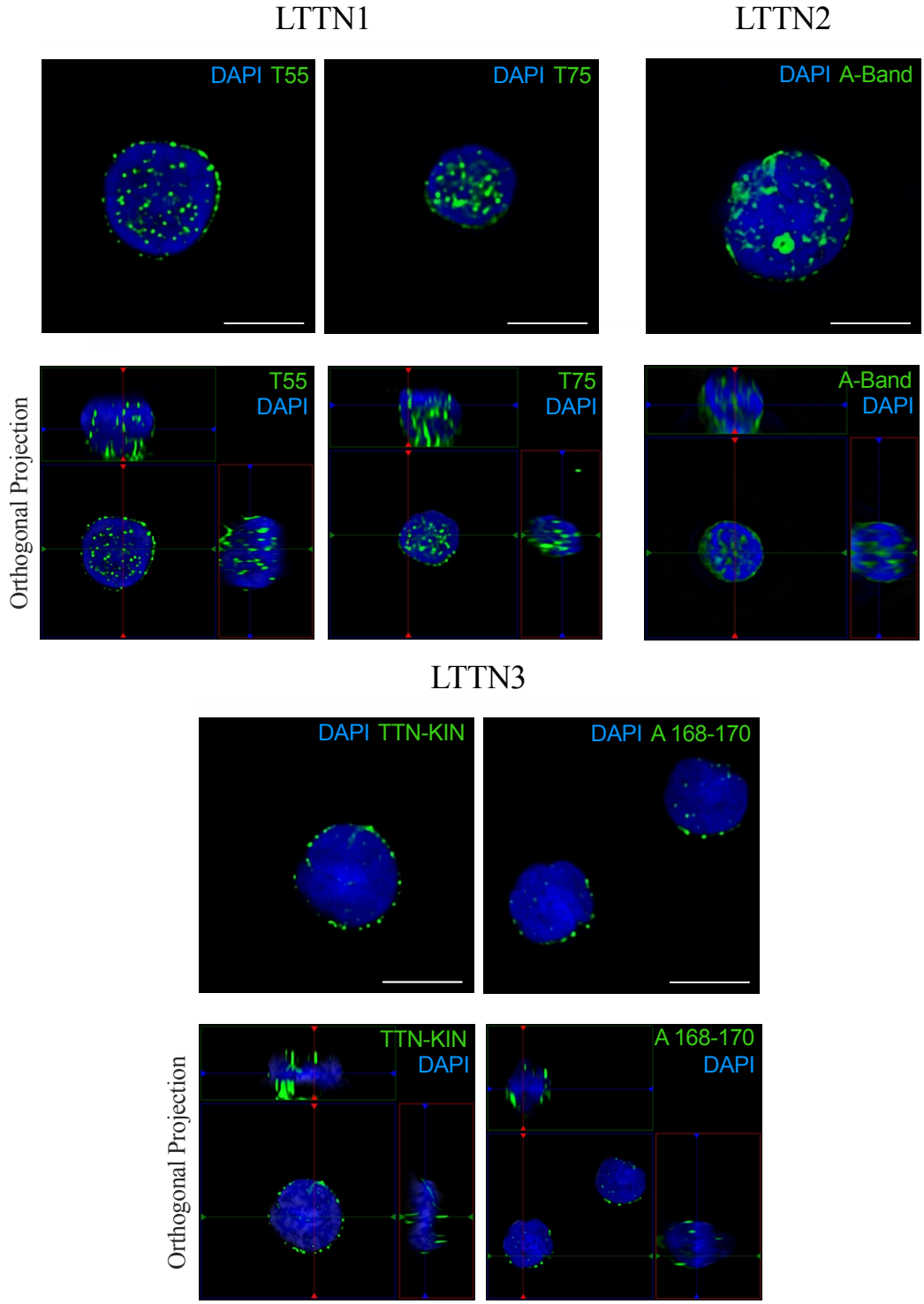

Fig. 7. Subcellular localization of LTTN1, LTTN2, and LTTN3. Fluorescence microscopy images of TTN isoform expression in human T lymphocytes assessed with TTN site-specific antibodies: T55 and T75 for LTTN1, A-Band for LTTN2, and TTN-Kin and A168-170 for LTTN3. The 3D Orthogonal projections show LTTN1, LTTN2, and LTTN3 subcellular localization in human T lymphocytes. TTN isoforms are shown in green, and the nucleus is stained with DAPI (blue). One representative experiment of four is shown. Scale bar: 5 µm.

2. Specific down-regulation of LTTN1 and LTTN3 expression in human primary T lymphocytes

To elucidate the role of the novel TTN isoforms in human lymphocyte physiology, we optimized a gene silencing technique individually targeting the two isoforms LTTN1 and LTTN3 in primary T lymphocytes. Considering the lack of specific chemical inhibitors, to investigate the potential involvement of LTTN1 and LTTN3 in primary T lymphocyte trafficking and physiology, we took advantage of an *RNA interference* technique by using a pool of four specific small interfering RNAs (siRNAs) selectively targeting either LTTN1 or LTTN3. Comparative tests showed that, in contrast to LTTN2 (data not shown), LTTN1 and LTTN3 were both amenable to the most effective silencing by siRNAs approach. Further experiments are, thus, needed to efficiently down-modulate the expression also of LTTN2 to study its role in T cell physiology.

Nucleoporation of human primary T lymphocytes with LTTN1- and LTTN3-specific siRNAs, efficiently diminished the intracellular content of these proteins in a time-dependent manner generating a cell population showing a 40-60% LTTN1 suppression within 5 days (Fig. 8A), and a mean decrease of about 50% in LTTN3 expression the fourth day after transfection (Fig. 8B). Lymphocytes nucleoporation with a pool of Scr siRNAs was ineffective.

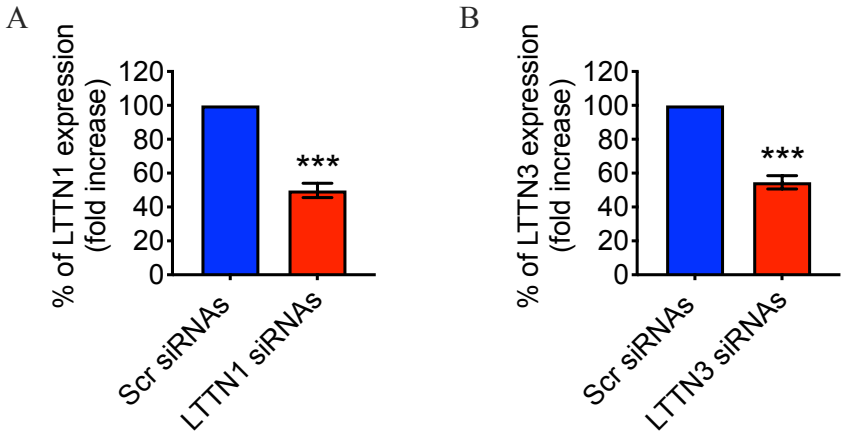

Fig. 8. LTTN1- and LTTN3-specific siRNAs mediate efficient protein down-regulation in human primary T lymphocytes. Flow Cytometry analysis of LTTN1 (**A**) and LTTN3 (**B**) expression in human primary T lymphocytes nucleoporated either with a pool of four Scr (control) or four LTTN1- and LTTN3-specific siRNAs and kept in culture

for 5 and 4 days respectively. **A** and **B**, Data were normalized to Scr siRNAs. Data are mean ± SD; Unpaired Student's t-test, ***P<0.001, (n=5).

Prior to evaluate the functional effects of LTTN1 and LTTN3 knock-down (KD) in T lymphocytes, we checked cell viability after 5 and 4 days transfection with LTTN1- and LTTN3-specific siRNAs, respectively. As is shown in Fig. 9A and 9B, both LTTN1 and LTTN3 silencing did not affect cell viability.

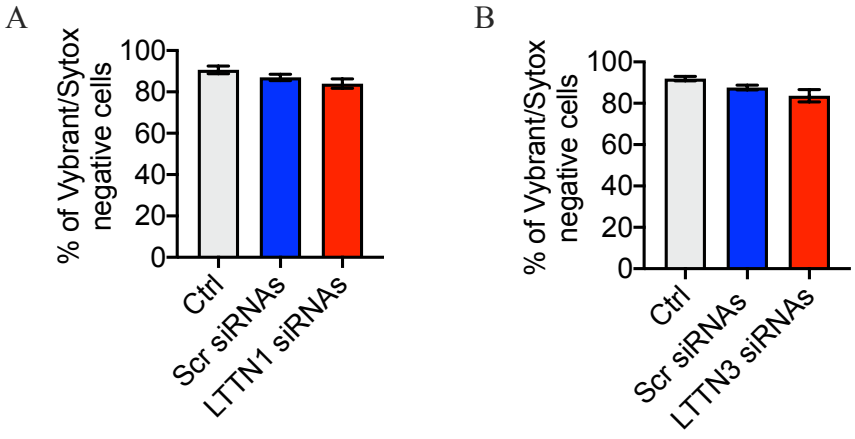

Fig. 9. LTTN1 and LTTN3 KD did not affect cell viability after transfection. Transfection of T lymphocytes either with Scr siRNAs or LTTN-specific siRNAs (**A**, LTTN1 siRNAs; **B**, LTTN3 siRNAs) did not affect cell viability in comparison with untreated cells (Ctrl) after 5 (**A**) and 4 (**B**) days transfection. Cell viability was measured by using Vybrant/Sytox viable dyes. Data are mean ± SD, (n=3).

3. Down-regulation of LTTN1 and LTTN3 impairs CXCL12-triggered rapid adhesion on ICAM-1 and VCAM-1

We, next, decided to evaluate the involvement of LTTN3 in chemokine-triggered T lymphocytes static adhesion mediated by LFA-1- and VLA-4. To exclude the possibility that the effect of LTTN3 silencing on integrin activation and leukocyte adhesion may be due to a down-regulation of specific pro-adhesive receptors, we checked the levels of β_2 and α_4 integrins and of CXCR4 chemokine receptor on LTTN3-silenced T lymphocytes. By comparing T cells nucleoporated with Scr siRNAs with cells nucleoporated with LTTN3-specific siRNAs, we found that,

down-regulation of LTTN3 did not affect the expression of these molecules (Fig. 10).

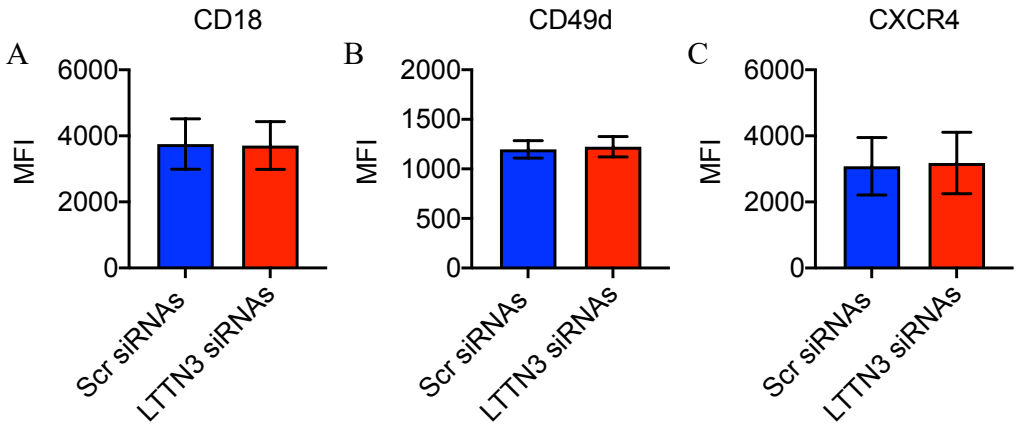

Fig. 10. LTTN3 down-regulation does not affect adhesion molecule expression. LTTN3-silenced T lymphocytes do not present differences in CD18 (**A**; β_2 integrins), CD49d (**B**; α_4 integrins), and CXCR4 (**C**) expression in comparison with cell nucleoporated with Scr siRNAs. Data are mean ± SD. Unpaired Student's t-test, (n=4).

By performing static adhesion assay on ICAM-1 and VCAM-1, we have been able to observe that LTTN3 down-regulation in T lymphocytes led to strong reduction in the number of ICAM-1- and VCAM-1-adherent cells upon CXCL12 stimulation, in comparison with cells nucleoporated with Scr siRNAs (Fig. 11A and 11B). The same results were previously obtained for LTTN1-silenced T cells. Indeed, T cells down-regulated in LTTN1 expression, presented a robust impairment in LFA-1- and VLA-4-mediated adhesion on ICAM-1 and VCAM-1, respectively, upon CXCL12 stimulation (Fig. 11C and 11D).

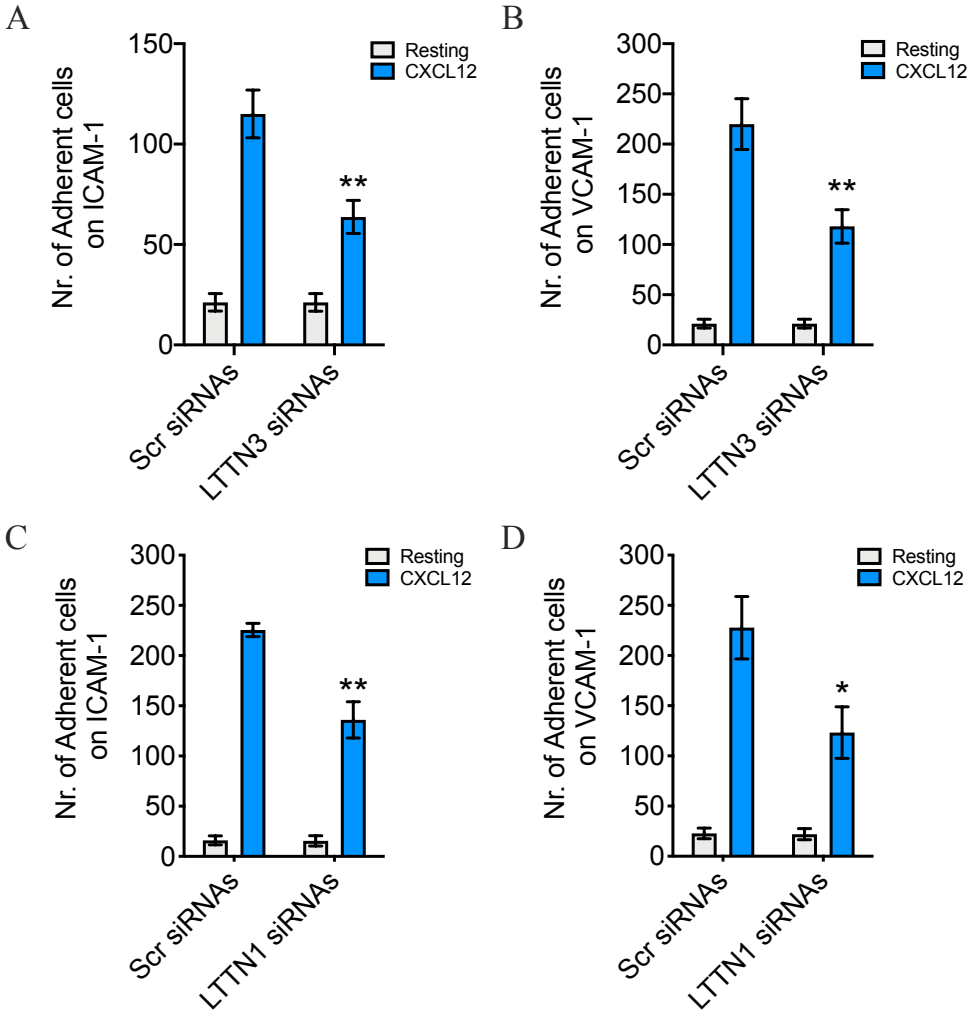

Fig. 11. CXCL12-dependent rapid adhesion is reduced after LTTN3 or LTTN1 down-regulation in T lymphocytes. Static adhesion assay on ICAM-1 or VCAM-1 of human primary T lymphocytes nucleoporated either with Scr siRNAs or LTTN3- (**A** and **B**) or LTTN1-specific siRNAs (**C** and **D**), stimulated with buffer (resting) or with CXCL12. Data are mean ± SD. Unpaired Student's t-test, *P<0.05, **P<0.01, (n=5).

4. LTTN3 down-regulation, as well as LTTN1 down-regulation, prevents CXCL12-triggered activation of RhoA and Rac1

In previous studies we have demonstrated that, in human primary T lymphocytes, the small GTPases RhoA and Rac1, by activating the downstream effectors PLD1 and PIP5K1C, mediate LFA-1 activation by CXCL12. Data from LTTN1 isoform analysis showed that LTTN1 silencing prevented CXCL12-triggered activation of both RhoA and Rac1 small GTPases by ~70% and ~80% respectively (Fig. 12A

and 12B, respectively). Consistent with these findings, LTTN1 down-regulation also reduced CXCL12-induced LFA-1 transition to heterodimeric high-affinity state (Fig. 12C). Thus, we set out to test whether also LTTN3 could be involved in the rapid activation of the Rho module by CXCL12 in human primary T lymphocytes.

In specific G-LISA assay we observed that down-regulation of LTTN3 expression reduced activation of both RhoA (Fig. 12D) and Rac1 (Fig. 12E) triggered by CXCL12, without interfering with total RhoA and Rac1 expression (Fig. 12G and 12H, respectively). Accordingly, LTTN3 silencing decreased CXCL12-induced LFA-1 transition to heterodimeric intermediate-affinity state (Fig. 12F).

These data suggest that, in addition to LTTN1, also LTTN3 isoform seems to be involved in the upstream activation of RhoA and Rac1 small GTPases, thus mediating CXCL12-triggered activation of the Rho module.

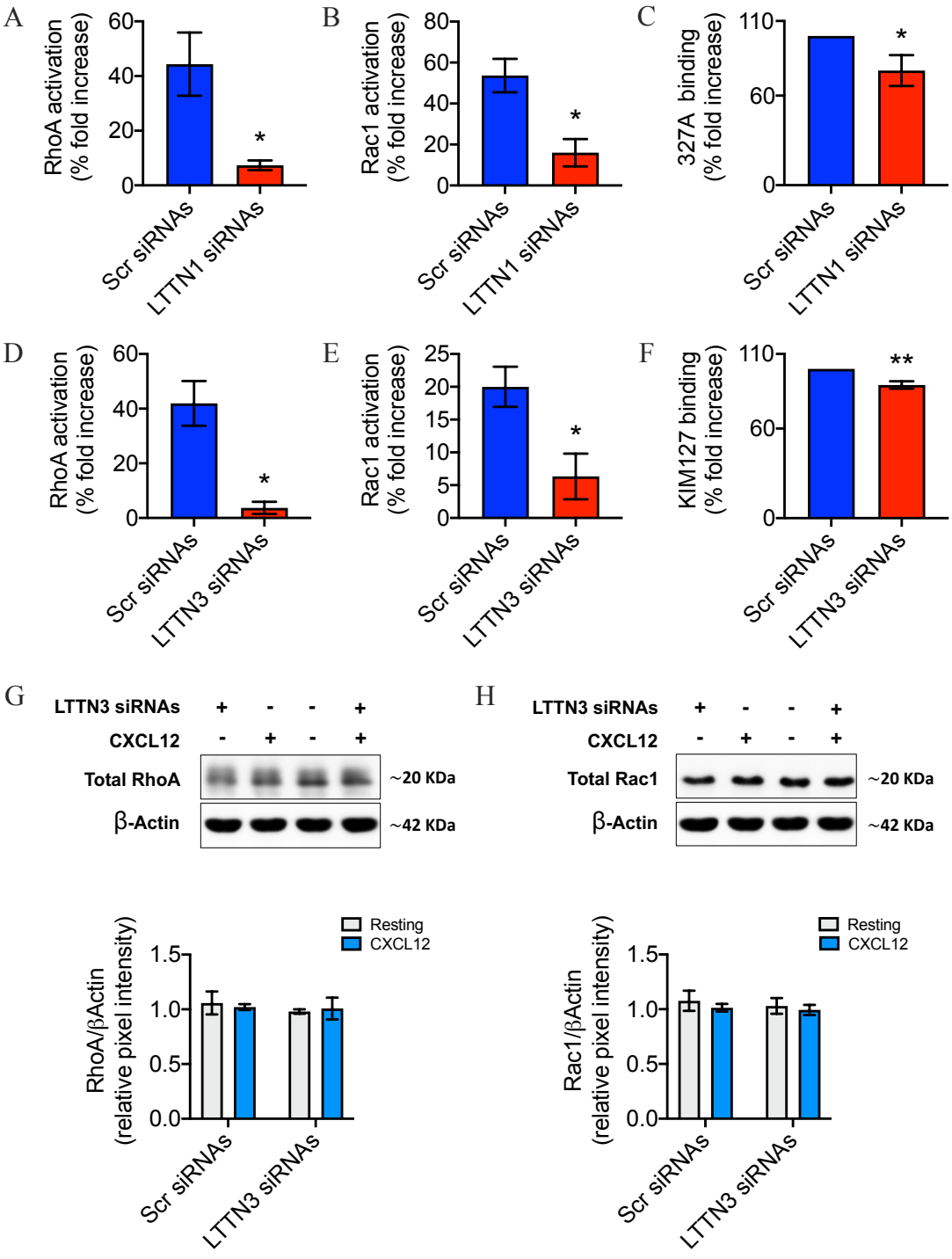

Fig. 12. CXCL12-triggered activation of RhoA and Rac1 is prevented by LTTN3 down-modulation. A, **B**, G-LISA assay detecting RhoA (**A**) and Rac1 (**B**) activation in human primary T lymphocytes nucleoporated either with Scr or LTTN1-specific siRNAs. **C**, T lymphocytes nucleoporated either with Scr or LTTN1-specific siRNAs, were stimulated for 120 s with buffer or 0.05 µM CXCL12 under stirring in the presence of 327A. **D**, **E**, G-LISA assay detecting RhoA (**D**) and Rac1 (**E**) activation in human primary T lymphocytes nucleoporated either with Scr or LTTN3-specific siRNAs. **F**, T

lymphocytes nucleoporated either with Scr or LTTN3-specific siRNAs, were stimulated for 120 s with buffer or 0.05 µM CXCL12 in the presence of KIM127. **G**, **H**, Immunoblot and densitometric quantification of total RhoA (**G**) and Rac1 (**H**) in human primary T lymphocytes nucleoporated either with Scr siRNAs or LTTN3-specific siRNAs, stimulated with buffer (Resting) or with CXCL12. Data are mean ± SD. Unpaired Student's t-test, *P<0.05, **P<0.01, (n=3).

5. LTTN1 and LTTN3 have an opposite role in chemokine-triggered T lymphocyte migration

Our previous data on LTTN1 showed that, in transwell migration assays, LTTN1 silencing potentiated T cells migration triggered by CXCL12 through 3 µm pores (Fig. 13A). The involvement of LTTN1 in the regulation of actin cytoskeleton dynamics was excluded since protein silencing did not affect the basal content of F-actin, nor the increase in F-actin triggered by CXCL12. Thus, we speculated that T lymphocytes must decrease their content in LTTN1 to decrease their stiffness and facilitate their migration across small gaps. Next, we asked whether also LTTN3 could be involved in T cell migration, and we performed transwell migration assays with LTTN3-silenced cells. Unlike LTTN1, we found that down-regulation of the smallest isoform, decreased cells migration triggered by CXCL12 through 3 µm pores (Fig. 13B). Therefore, LTTN3 seems to have a different role, compared to LTTN1, in T cells migration. Indeed, while LTTN1 should be degraded by the cell to migrate, the presence of LTTN3 is likely required to mediate chemokine-induced migration.

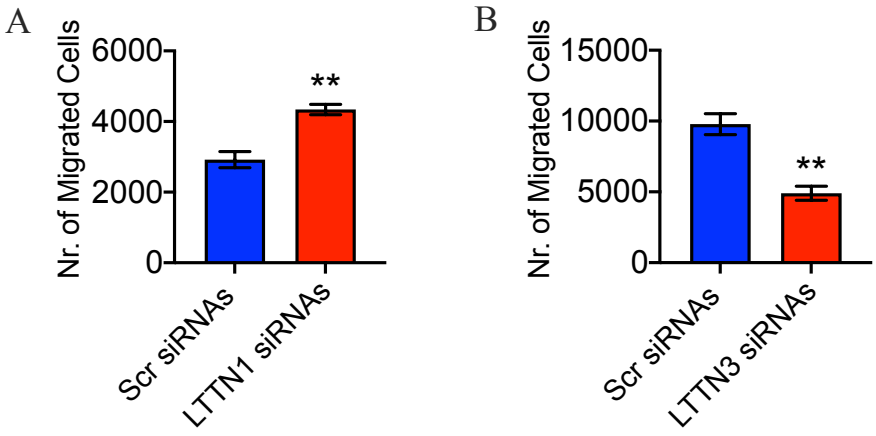

Fig. 13. Unlike LTTN1, LTTN3 is a positive regulator of CXCL12-triggered T lymphocytes migration. Transwell migration assay through 3 µm pores of human primary T lymphocytes nucleoporated either with Scr siRNAs or LTTN1- (**A**) or LTTN3-specific (**B**) siRNAs. Data are mean ± SD. Unpaired Student's t-test, **P<0.01, (n=3).

6. LTTN1 preserves the cellular integrity of T lymphocytes in the microcirculation

Previous data from our laboratory suggest that LTTN1 deficiency could affect the survival of T lymphocytes in microcirculation, where mechanical stress due to passive deformation induced by crossing capillary nets continuously occurs. Indeed, *in vitro* studies performed on a microfluidic device consisting of parallel microchannels with diameters narrower than the average human lymphocytes, demonstrated that the LTTN1-silenced cells were unable to pass through the microfluidic channels and were destroyed immediately after crossing the initial microchannel constriction. On the contrary, cells nucleoporated with Scr siRNAs were able to cross the microchannels as easily as non-treated cells.

Thus, to test this hypothesis *in vivo*, we exploited an intravital microscopy setting by injecting intravenously in mice T cells nucleoporated with Scr siRNAs (controls) or with LTTN1-specific siRNAs. After 30 min we check the relative abundance of control and silenced cells in the vessels of not perfused lungs. We alternatively labeled the cells of the two conditions with different fluorochromes to reveal possible non-specific effects.

Fluorescence microscopy analysis showed a clear imbalance between control cells and LTTN1-silenced cells in the lung vasculature of different pulmonary lobes,

with a consistent loss of silenced cells in comparison with controls (Fig. 14A and 14B). Pooled image quantification data from all lobes and lungs analyzed showed an overall reduction of ~54% in the number of LTTN1-silenced T cells (Fig. 14C).

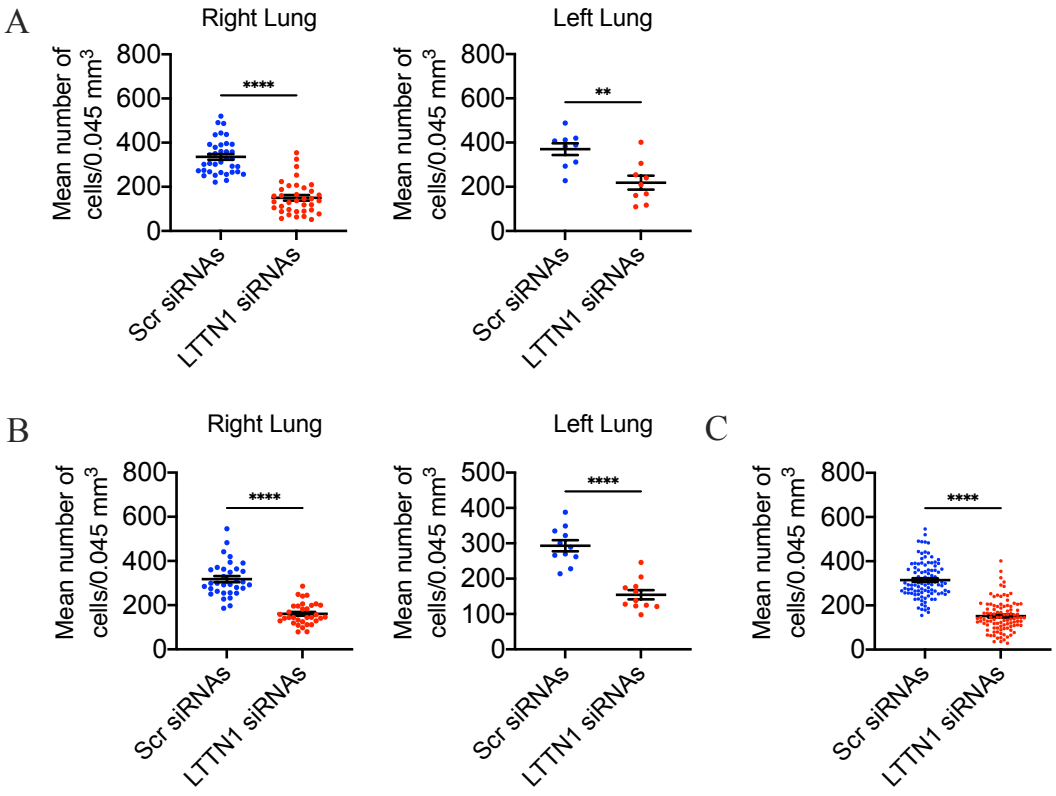

Fig. 14. LTTN1 down-regulation impairs cellular integrity of T lymphocytes in mouse lung vasculature. Permanence of human T lymphocytes in mouse blood circulation deduced from the mean number of cells per volume of pulmonary tissue. Dots represent individual analyzed images. **A**, Scr siRNAs-transfected cells (CMTMR) and LTTN1-silenced cells (CMTPX). **B**, Scr siRNAs-transfected cells (CMTPX) and LTTN1-silenced cells (CMTMR). **C**, Aggregated data from panels **A** and **B**. Data are mean ± SEM. Unpaired Student's t-test, **P<0.01, ****P< 0.001.

Moreover, we also performed flow cytometry analysis on mouse blood and lung lysates after the intravenous injection in mice of T cells nucleoporated with Scr siRNAs and with LTTN1-specific siRNAs. In agreement with the microscopy data, quantification of the relative number of fluorescently labelled cells, both in blood samples and in lung lysates, evidenced a significant reduction of LTTN1-silenced T cells with respect to control cells (Fig. 15A).

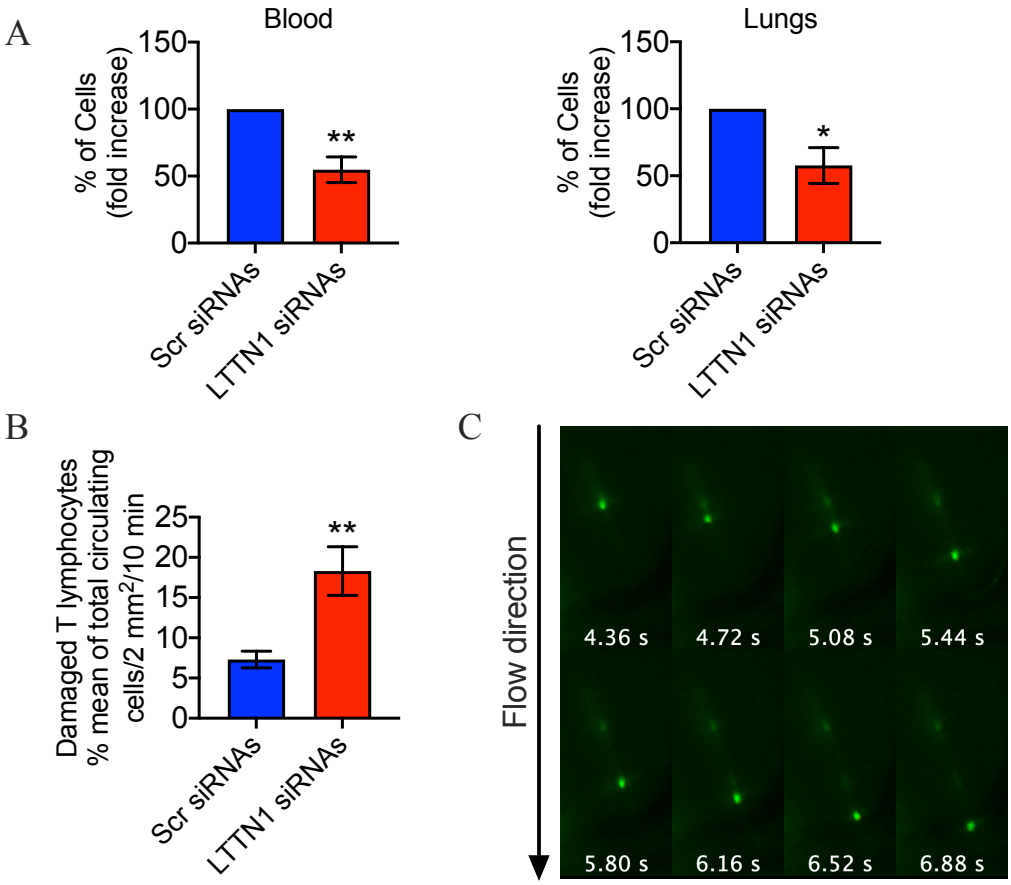

Fig. 15. LTTN1 down-regulation impairs cellular integrity of T lymphocytes in mouse lung vasculature. Permanence of human T lymphocytes nucleoporated with Scr siRNAs or with LTTN1-specific siRNAs in mouse blood and in lung lysates (**A**); mouse was euthanized after 30 min from the injection. Control (Scr siRNAs) and LTTN1-silenced cells were alternatively labeled with CMAC and CMFDA and data were merged in the same plot. Data were normalized to Scr siRNAs. Unpaired Student's t-test, *P<0.05, **P<0.01, (n=5). **B**, Quantification of cells manifesting a progressive intravascular rear release of cellular labeled content (AO) in control (Scr siRNAs) and LTTN1-silenced human T lymphocytes. Data are % means in 6 fields from three experiments ± SEM. Unpaired Student's t-test, **P<0.01. **C**, Fluorescence microscopy images of AO labeled LTTN1-silenced human T lymphocyte entrapped in the microcirculation and manifesting a progressive intravascular rear release of cell AO labeled content. Shown is a temporal sequence of about 2.5 seconds. One representative cell from three experiments is shown.

Lastly, to directly assess in real time the resilience of LTTN1-silenced T lymphocytes to passive deformation occurring in the microcirculation, we decided to apply an established intravital microscopy setting to directly visualize the microcirculation within muscle vasculature, where an extensive texture of parallel capillaries is present [44–46]. We injected fluorescently labeled T lymphocytes, either nucleoporated with Scr siRNAs or with LTTN1-specific siRNAs, directly in the

mouse right carotid, thus allowing immediate arrival of the cells into the pectoral muscle vasculature, avoiding previous passage through other organs. We found that cells nucleoporated with Scr siRNAs progressively accumulate in the pectoral muscle microcirculation at early time points (~5 min) and remain entrapped for a prolonged time (~20 min). In contrast, LTTN1-silenced cells accumulated in the microcirculation similarly to control cells at early time points (~5 min), but progressively disappeared at late time points (~20 min). This was not exclusively due to cell disengagement from the microcirculation to come back to the blood flow; indeed, frame-by-frame video analysis showed that, compared to control cells, almost three times higher percentage of LTTN1-silenced cells manifested, with respect to the blood flow direction, a progressive intravascular rear leakage of cell fluorescent content, a morphology indicating cell damage under flow (Fig. 15B and 15C).

Altogether, these data are in keeping with the previous *in vitro* experiments and indicate that LTTN1 provides circulating T lymphocytes the resilience to mechanical stress induced by passive deformation in the microcirculation.

7. LTTN1 and ERM proteins concurrently control microvilli structure and function

Recent data from our laboratory demonstrated that, in the context of the canonical steps of leukocyte recruitment, silencing of LTTN1 impaired the ability of T lymphocytes to establish under flow adhesive interactions at physiologic shear stress (2 dynes/cm^2) on both E-selectin and P-selectin suggesting functional defects in L-selectin and PSGL-1. Since L-selectin and PSGL-1 expressions were unaffected in LTTN1-silenced cells and given the well-known critical role of plasma membrane microvilli in cell capturing and rolling, it has been hypothesized that the impairment of cell capturing under flow conditions was due to a deficiency of microvilli. This was confirmed by scanning electron microscopy (SEM), which showed that LTTN1 silencing induced the collapse of microvilli in T lymphocytes. Since microvilli stability is dependent on the phosphorylation state of ERM proteins [37], with Rac1 mediating chemokine triggered ERM dephosphorylation leading to

microvilli collapse [38], we investigated whether LTTN1 could control the phosphorylation state of ERM proteins. As expected, CXCL12 triggered rapid dephosphorylation of Ezrin and Moesin, the two main ERM proteins in lymphocytes, followed by recovery within 10-30 min (Fig. 16A, 16B, and 16C). However, LTTN1 silencing did not affect chemokine-triggered dephosphorylation of ERMs proteins (Fig. 16D, 16E, and 16F). Importantly, ERM protein phosphorylation was also unaffected by LTTN1 silencing in absence of any chemokine signaling (Fig. 16B and 16D, resting columns), suggesting that LTTN1 controls microvilli stability independently of the phosphorylation state of ERM proteins.

These data show that LTTN1 directly controls the morphogenesis of microvilli and explains the defective capturing and rolling of LTTN1-silenced T lymphocytes under flow condition.

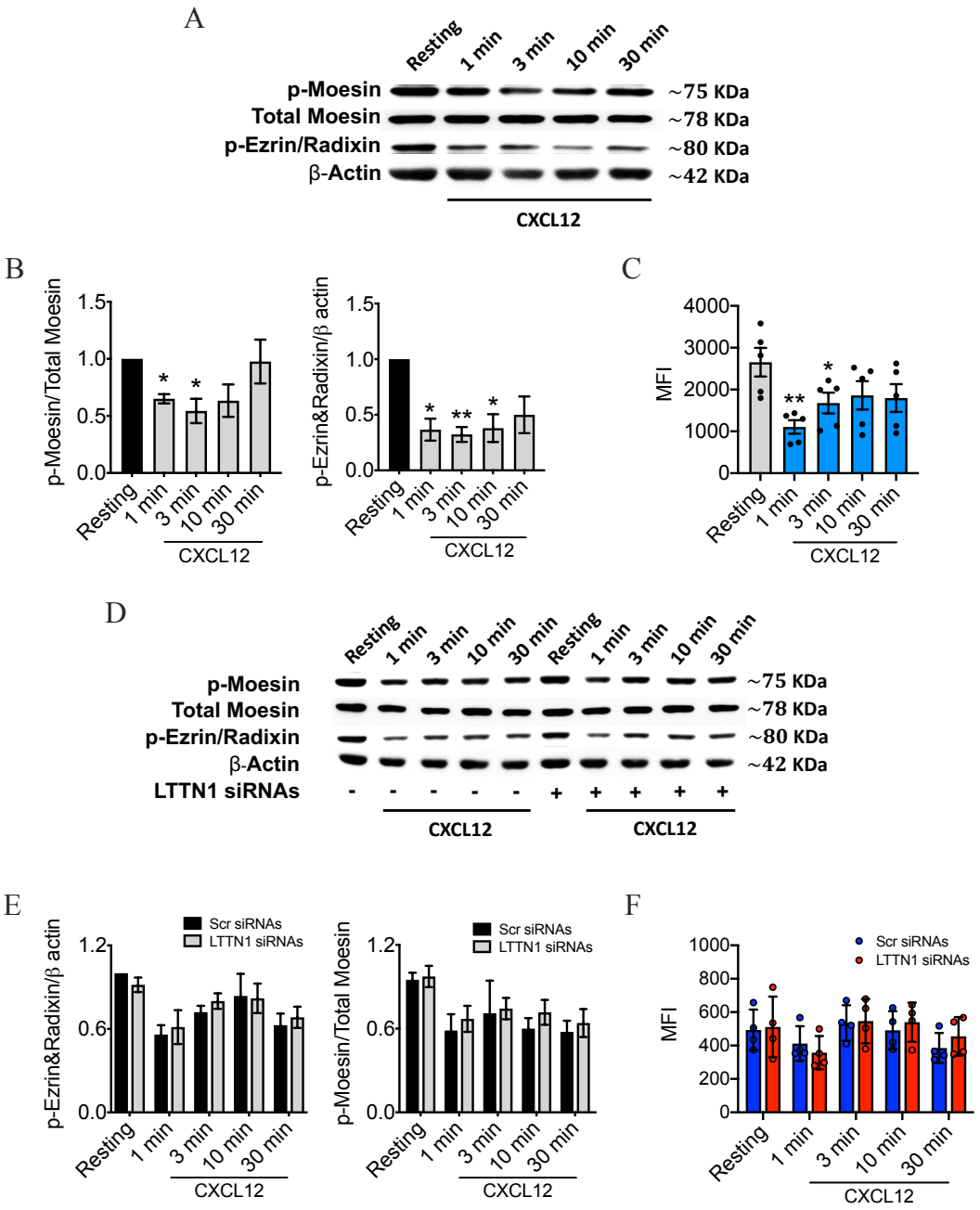

Fig. 16. LTTN1 silencing does not affect the phosphorylation state of ERM proteins. **A**, **B**, immunoblot evaluation (**A**) and quantification (**B**) of p-Moesin, Total Moesin, and p-Ezrin/Radixin in T lymphocytes stimulated with buffer (Resting) or with 200 nM CXCL12. **C**, flow cytometry evaluation of p-ERMs expression in cells as in panel **A**. Data are means ± SEM. Unpaired Student's t-test, *P< 0.05, **P<0.01, (n=5). **D**, **E**, immunoblot evaluation (**D**) and quantification (**E**) of p-Moesin, Total Moesin, and p-Ezrin/Radixin in T lymphocytes nucleoporated with a pool of four Scr or four LTTN1-specific siRNAs, kept in culture for 5 days, and stimulated as in panel **A**. **F**, flow cytometry evaluation of p-ERMs expression in cells as in panel **D**. Data are means ± SEM. ANOVA followed by Tukey's test, (n=4). In **A** and **D**, one representative experiment of three is shown.

DISCUSSION

During the immune response, leukocytes integrate a number of microenvironmental signals which are concurrently processed by mechano-transduction mechanisms [47–53]. Circulating leukocytes must also cope with both passive and active cell deformation, respectively generated by the incessant passage across capillary nets and, during migration, by the adaption of cell body and nucleus to the small gaps between endothelial cells and within the extracellular matrix 3-dimensional meshwork [25,28,54–56]. Therefore, trafficking leukocytes need to simultaneously control pathways of mechano-transduction and resilience to mechanical stress. Thus, we hypothesized the existence of coordinated molecular mechanisms of regulation of these events inside the cell.

Detergent-resistant membrane domains have provided a structural context to understand the topography and organization of signaling mechanisms and have been widely implicated in many aspects of leukocyte physiology [57,58]. Consequently, we postulated that DRMs could provide anchoring to proteins that concurrently coordinate mechano-signaling and resilience to mechanical stress in human primary leucocytes.

The analysis of DRMs isolated from human primary T lymphocytes by mass spectrometry identified 82 proteins including titin, the largest protein encoded by the human genome and mainly known to determine sarcomeric viscoelasticity, contributing to muscle cells passive stiffness [5]. The functional, structural, interactomic, and topological characteristics of TTN make it an ideal candidate coordinator of mechano-transduction and cell stiffness in human T lymphocytes. The MS data, confirmed by RNA-seq analysis and subsequent PCR, revealed the existence of three novel TTN isoforms in T lymphocytes, altogether encompassing the entire *TTN* gene. These isoforms were named LTTN1, LTTN2, and LTTN3. Furthermore, LTTN1 and LTTN2 were detected by MS analysis in T lymphocyte DRMs, but not LTTN3. Since DRMs are nanoscale structures, the much larger LTTN1 and LTTN2 isoforms, estimated to be 300 and 620 nm in size, are unlikely to be confined within them. Thus, it is possible that LTTN1 and LTTN2 extend from DRMs into the cell interior. Notably, LTTN1 and LTTN2 show protein

domain arrangements like canonical TTN, suggesting interactome properties comparable to those of muscle TTN. Thus, we hypothesized that T lymphocyte DRMs can be anchors for LTTN1 and LTTN2, and that these isoforms extend from DRMs into the cell, generating an intracellular mechano-scaffolding skeleton that control the signaling and mechanic properties of human T cells. Indeed, 3D image analysis revealed distinct intracellular distribution for each isoform, with LTTN3 confined to the cytosol whereas LTTN1 and LTTN2 localized to both nucleus and cytosol and thus, possibly anchored to DRMs.

Taken together, the previous results obtained from our laboratory on LTTN1 and the new data concerning LTTN3, give an important role to these proteins in T cell trafficking. Indeed, by means of the molecular approach of LTTN1 and LTTN3 silencing based on a pool of isoform-specific siRNAs, we demonstrated that down-regulation of these isoforms in T lymphocytes impairs CXCL12-triggered rapid LFA-1- and VLA-4-mediated adhesion on ICAM-1 and VCAM-1, respectively. Furthermore, both LTTN3 and LTTN1 silencing reduced CXCL12-induced transition to heterodimeric intermediate- and high-affinity state, respectively. This was in keeping with the data showing that LTTN1 and LTTN3 silencing prevents both RhoA and Rac1 activation by CXCL12.

Because LTTN1 lacks kinase activity, which in T lymphocytes is possibly restricted to the LTTN3 isoform, it is likely that LTTN1 regulates integrin activation via docking-scaffolding mechanisms. However, even if some studies have attributed a catalytic activity to the kinase domain of muscular titin, recent findings reveal that TK is an inactive pseudokinase with mechanosensing properties exerted trough scaffolding activity [9]. Thus, it could be possible that also in T lymphocytes the kinase domain of LTTN3 lacks catalytic activity. LTTN3 could participate in cell signaling translating extracellular stimuli into regulatory pathways through scaffolding activity. It has been previously shown that at least four rho GEF domains mediate the CXCL12-triggered activation of rho GTPases, concurrently regulated by JAK and BTK protein tyrosine kinases [31,32,59]. LTTN1 and LTTN3 could regulate the activity of these intermediates in the pathway leading to integrin activation.

Cell migration requires coordination of cytoskeletal dynamics and reorganization, and intracellular signal transduction to reduce cell stiffness to favor deformability [60,61]. LTTN1 silencing facilitates cell migration whereas, in contrast, LTTN3 down-regulation plays the opposite role. Indeed, we found that LTTN3 silencing prevents cell migration across small gaps. Results from our previous study showed that LTTN1 is likely to regulate both passive and active cell deformability and that is rapidly degraded in a calpeptin-sensitive manner by either chemokine or integrin signaling. This revealed an inverse correlation between LTTN1 expression and the activity of pro-adhesive mediators controlling cell polarization, spreading, and motility, which are characterized by increased cell plasticity [61–63]. Indeed, since cells that cannot degrade LTTN1 are unable to squeeze through and overstep small gaps, LTTN1 appears to be a negative regulator of cell plasticity. Moreover, LTTN1-silenced T lymphocytes presented a compromised resilience to passive cell deformation, with both the cell body and nucleus destroyed by passive mechanical stress *in vitro*. Also, the resilience of T lymphocytes to osmotic shock was affected by LTTN1 deficiency. Thus, it is likely that LTTN1 down-modulation may occur to reduce cell stiffness and favor cell deformability. On the other hand, considering that down-modulation of LTTN3 leads to impaired cell migration through small gaps, this clearly suggests that maintenance of LTTN3 expression is fundamental to promote chemokine-triggered T cell migration. This establishes a clear dichotomy in the regulatory role of these two novel TTN isoforms, with LTTN3 possibly restricted to a signaling role, whereas LTTN1 involved in both signaling and mechanical role.

The new *in vivo* data confirmed the putative role of LTTN1 in providing circulating T lymphocytes resilience to mechanical stress induced by passive deformation in the microcirculation. Indeed, we found that LTTN1-silenced T lymphocytes injected either intravenously or in the carotid of the mouse were destroyed in the animal circulation within 30 min. These findings are in keeping with the previous *in vitro* experiments and indicate that LTTN1 regulates passive cell deformability, ensuring the survival of T lymphocytes in the bloodstream.

Recently we found that LTTN1 controls the canonical steps of T lymphocyte adhesion under flow conditions. Selectin-mediated rolling on both E-selectin and

P-selectin was impaired in LTTN1-silenced T cells which, however, did show unaffected PSGL-1 and L-selectin expression. Furthermore, we showed that cells down-regulated in LTTN1 expression lost the surface microvilli. Thus, given the well-known critical role of plasma membrane microvilli in capturing and rolling [64], we hypothesized that the impairment of cell capturing under flow conditions was due to a deficiency of microvilli. Interestingly, LTTN1 silencing did not affect the chemokine-triggered dephosphorylation of ERM proteins. This could possibly contrast with the reported role of Rac1 in the dephosphorylation of ERMs proteins induced by chemokines [38]. However, since LTTN1 silencing did not entirely abolish Rac1 activation, it is possible that the residual Rac1 activity is sufficient to mediate ERM protein dephosphorylation induced by chemokines in LTTN1-silenced cells. Importantly, however, in absence of any chemokine signaling, constitutive ERM protein phosphorylation was completely unaffected by LTTN1 silencing, suggesting that LTTN1 may control microvilli structure independently of the phosphorylation state of ERM proteins. Overall, the data suggest that LTTN1 and ERM proteins concurrently control microvilli structure and function and that chemokines may lead to microvilli collapse by simultaneously triggering Rac1-mediated ERM protein dephosphorylation and calpain-mediated LTTN1 degradation. It is known that TTN interacts with actin and actin-binding proteins in muscle cells [2,3,65]. Accordingly, it could be possible that LTTN1 may form an intracellular meshwork beneath the plasma membrane, anchoring actin-binding proteins, or the actin cytoskeleton backbone within the microvilli. The actin backbone may lose support because of LTTN1 degradation, causing the microvilli to collapse. Notably, microvilli are now recognized as sites of receptor aggregation and signal transduction [66]. Thus, besides their established role in leukocyte capturing and rolling, the critical role of LTTN1 in the morphogenesis of microvilli may provide new insights into their homeostasis and function.

Taken together, the previous and the new findings could suggest a LTTN1-centric model of T lymphocyte trafficking. In this model, circulating T lymphocytes rely on LTTN1 to maintain the stiffness to cope with passive deformation in the microcirculation. LTTN1 may ensure the survival of circulating cells until a permissive endothelium is engaged. Here, LTTN1 is critical to maintain microvilli,

allowing the presentation of the molecules required for cell capturing and rolling. In keeping with the role of TTN in muscle cell stiffness and with our data, LTTN1 degradation is essential at this stage to reduce stiffness increasing cell plasticity. LTTN1 degradation could also be necessary to reduce nuclear stiffness, thus allowing the nucleus to adapt to small gaps. During chemotaxis LTTN1 expression is kept low by concurrent inside-out and outside-in signaling generated by chemokines and integrins. Eventually, T lymphocytes may come back to circulation, where stiffness must be restored to ensure resilience to passive deformation. On the other hand, our preliminary results on LTTN3 suggest a role for this isoform as a modulator of chemokine-induced signal transduction. Indeed, in contrast with LTTN1, the down-regulation of this protein during chemotaxis impairs cell migration through small pores. This suggests that this isoform is unlikely subjected to degradation to reduce cell stiffness and increase deformability as LTTN1. Instead, as for muscle titin, LTTN3 could be a crucial signaling hub for proteins implicated in the *inside-out* and *outside-in* signaling pathways defining each step of leukocyte trafficking. Accordingly, LTTN3 also mediates chemokine-induced integrin activation and rapid cell adhesion.

However, further investigations are needed to better understand the functional contribution of LTTN3 in T lymphocyte physiology. It will be important to establish whether the kinase domain of LTTN3 has catalytic activity or if its role as pseudokinase is maintained in the context of the immune system. Moreover, other questions arise from this study, including the role of LTTN1 in T cell receptor function, which is almost exclusively localized on microvilli [67], the possible cooperation of LTTN1 with molecules proposed to maintain cell and nuclear stiffness and shape, such as vimentin, the LINC complex, and lamins [61,68–72]. Furthermore, considering the proposed role of TTN in chromosome structure and segregation and the detected nuclear localization of LTTN1, it will be interesting to determine whether it may have a role in the regulation of T lymphocyte gene expression or maturation, as well as in cell proliferation and division in tumor context [73–75].

Certain diseases, such as pulmonary distress syndrome and acute leukemia, are characterized by alterations in leukocyte rigidity that result in diffuse intravascular

leukostasis [76–78]. The molecular basis of leukostasis is poorly defined, but the role of LTTN1 in the stiffness and survival of circulating T lymphocytes may provide a new avenue of research. Notably, the *TTN* gene allows extensive splicing, and many genetic variants have been identified [2,79]. Therefore, it will be of great interest to investigate whether variants of the newly identified lymphocyte TTN isoforms may occur in pathology.

BIBLIOGRAPHY

1. Gigli, M. *et al.* A Review of the Giant Protein Titin in Clinical Molecular Diagnostics of Cardiomyopathies. *Front Cardiovasc Med* **3**, (2016).
2. Chauveau, C., Rowell, J. & Ferreiro, A. A Rising Titan: TTN Review and Mutation Update. *Hum Mutat* **35**, 1046–1059 (2014).
3. Tskhovrebova, L. & Trinick, J. Titin: properties and family relationships. *Nat Rev Mol Cell Biol* **4**, 679–689 (2003).
4. Savarese, M. *et al.* The complexity of titin splicing pattern in human adult skeletal muscles. *Skelet Muscle* **8**, 11 (2018).
5. Linke, W. A. & Hamdani, N. Gigantic Business: titin properties and function through thick and thin. *Circ Res* **114**, 1052–1068 (2014).
6. Linke, W. A. Titin Gene and Protein Functions in Passive and Active Muscle. *Annu Rev Physiol* **80**, 389–411 (2018).
7. Raynaud, F. *et al.* Calpain 1-titin interactions concentrate calpain 1 in the Z-band edges and in the N2-line region within the skeletal myofibril. *FEBS Journal* **272**, 2578–2590 (2005).
8. Bogomolovas, J. *et al.* Titin kinase ubiquitination aligns autophagy receptors with mechanical signals in the sarcomere. *EMBO Rep* **22**, (2021).
9. Bogomolovas, J. *et al.* Titin kinase is an inactive pseudokinase scaffold that supports MuRF1 recruitment to the sarcomeric M-line. *Open Biol* **4**, 140041 (2014).
10. Puchner, E. M. *et al.* Mechanoenzymatics of titin kinase. *Proceedings of the National Academy of Sciences* **105**, 13385–13390 (2008).
11. Lange, S. *et al.* The Kinase Domain of Titin Controls Muscle Gene Expression and Protein Turnover. *Science (1979)* **308**, 1599–1603 (2005).
12. TTN - Titin - Homo sapiens (Human) | UniProtKB | UniProt. https://www.uniprot.org/uniprotkb/Q8WZ42/entry#disease_variants.
13. Wicklund, M. P. The Limb-Girdle Muscular Dystrophies. *CONTINUUM Lifelong Learning in Neurology* **25**, 1599–1618 (2019).
14. Toro, C. *et al.* Exome sequencing identifies titin mutations causing hereditary myopathy with early respiratory failure (HMERF) in families of diverse ethnic origins. *BMC Neurol* **13**, 1–14 (2013).
15. Jungbluth, H., Wallgren-Pettersson, C. & Laporte, J. Centronuclear (myotubular) myopathy. *Orphanet J Rare Dis* **3**, 26 (2008).

16. Al-Qusairi, L. & Laporte, J. T-tubule biogenesis and triad formation in skeletal muscle and implication in human diseases. *Skelet Muscle* **1**, 1–11 (2011).
17. Ceyhan-Birsoy, O. *et al.* Recessive truncating titin gene, TTN, mutations presenting as centronuclear myopathy. *Neurology* **81**, 1205 (2013).
18. Schultheiss, H. P. *et al.* Dilated cardiomyopathy. *Nat Rev Dis Primers* **5**, (2019).
19. Kellermayer, D., Smith, J. E. & Granzier, H. Titin mutations and muscle disease. *Pflugers Arch* **471**, 673–682 (2019).
20. Taylor, M. *et al.* Genetic Variation in Titin in ARVC-Overlap Syndromes. *Circulation* **124**, 876 (2011).
21. Peled, Y. *et al.* Titin Mutation in Familial Restrictive Cardiomyopathy. *Int J Cardiol* **171**, 24–30 (2014).
22. Hackman, P., Savarese, M., Carmignac, V., Udd, B. & Salih, M. A. Salih Myopathy. *GeneReviews* (2019).
23. Carmignac, V. *et al.* C-Terminal Titin Deletions Cause a Novel Early-Onset Myopathy with Fatal Cardiomyopathy. *Ann Neurol.* (2007) doi:10.1002/ana.21089.
24. Chauveau, C. *et al.* Recessive TTN truncating mutations define novel forms of core myopathy with heart disease. *Hum Mol Genet* **23**, 980 (2014).
25. Ley, K., Laudanna, C., Cybulsky, M. I. & Nourshargh, S. Getting to the site of inflammation: the leukocyte adhesion cascade updated. *Nature Reviews Immunology 2007 7:9* **7**, 678–689 (2007).
26. Laudanna, C. & Bolomini-Vittori, M. Integrin activation in the immune system. *Wiley Interdiscip Rev Syst Biol Med* **1**, 116–127 (2009).
27. von Andrian, U. H., Hasslen, S. R., Nelson, R. D., Erlandsen, S. L. & Butcher, E. C. A central role for microvillous receptor presentation in leukocyte adhesion under flow. *Cell* **82**, 989–999 (1995).
28. Nourshargh, S. & Alon, R. Leukocyte Migration into Inflamed Tissues. *Immunity* **41**, 694–707 (2014).
29. Kinashi, T. Intracellular signalling controlling integrin activation in lymphocytes. *Nat Rev Immunol* **5**, 546–559 (2005).
30. Laudanna, C. & Alon, R. Right on the spot. Chemokine triggering of integrin-mediated arrest of rolling leukocytes. *Thromb Haemost* **95**, 5–11 (2006).
31. Toffali, L., Montresor, A., Mirenda, M., Scita, G. & Laudanna, C. SOS1, ARHGEF1, and DOCK2 rho-GEFs Mediate JAK-Dependent LFA-1 Activation by Chemokines. *J Immunol* **198**, 708–717 (2017).

32. Montresor, A. *et al.* JAK tyrosine kinases promote hierarchical activation of Rho and Rap modules of integrin activation. *J Cell Biol* **203**, 1003–1019 (2013).
33. Evans, R. *et al.* Integrins in immunity. *J Cell Sci* **122**, 215–225 (2009).
34. Shulman, Z. *et al.* Lymphocyte Crawling and Transendothelial Migration Require Chemokine Triggering of High-Affinity LFA-1 Integrin. *Immunity* **30**, 384 (2009).
35. Tsukita, S. & Yonemura, S. Cortical Actin Organization: Lessons from ERM (Ezrin/Radixin/Moesin) Proteins. *J Biol Chem* (1999) doi:10.1074/jbc.274.49.34507.
36. Bretscher, A., Edwards, K. & Fehon, R. G. ERM proteins and merlin: integrators at the cell cortex. *Nat Rev Mol Cell Biol* **3**, 586–599 (2002).
37. Brown, M. J. *et al.* Chemokine stimulation of human peripheral blood T lymphocytes induces rapid dephosphorylation of ERM proteins, which facilitates loss of microvilli and polarization. *Blood* **102**, 3890–3899 (2003).
38. Nijhara, R. *et al.* Rac1 mediates collapse of microvilli on chemokine-activated T lymphocytes. *J Immunol* **173**, 4985–4993 (2004).
39. von Andrian, U. H., Hasslen, S. R., Nelson, R. D., Erlandsen, S. L. & Butchert, E. C. A Central Role for Microvillous Receptor Presentation in Leukocyte Adhesion under Flow. *Cell* **82**, 989–999 (1995).
40. Ghosh, S. *et al.* CCR7 signalosomes are preassembled on tips of lymphocyte microvilli in proximity to LFA-1. *Biophys J* **120**, 4002–4012 (2021).
41. Greicius, G. *et al.* Microvilli structures on B lymphocytes: Inducible functional domains? *Int Immunol* **16**, 353–364 (2004).
42. Orbach, R. & Su, X. Surfing on Membrane Waves: Microvilli, Curved Membranes, and Immune Signaling. *Front Immunol* **11**, (2020).
43. Ghosh, S. *et al.* ERM-Dependent Assembly of T Cell Receptor Signaling and Co-stimulatory Molecules on Microvilli prior to Activation. *Cell Rep* **30**, 3434-3447.e6 (2020).
44. Torrente, Y. *et al.* Intraarterial Injection of Muscle-Derived Cd34+Sca-1+ Stem Cells Restores Dystrophin in mdx Mice. *J Cell Biol* **152**, 335 (2001).
45. Torrente, Y. *et al.* Identification of a putative pathway for the muscle homing of stem cells in a muscular dystrophy model. *J Cell Biol* **162**, 511 (2003).
46. Gavina, M. *et al.* VCAM-1 expression on dystrophic muscle vessels has a critical role in the recruitment of human blood-derived CD133+ stem cells after intra-arterial transplantation. *Blood* **108**, 2857–2866 (2006).

47. Kechagia, J. Z., Ivaska, J. & Roca-Cusachs, P. Integrins as biomechanical sensors of the microenvironment. *Nature Reviews Molecular Cell Biology* vol. 20 457–473 Preprint at https://doi.org/10.1038/s41580-019-0134-2 (2019).
48. Martino, F., Perestrelo, A. R., Vinarský, V., Pagliari, S. & Forte, G. Cellular mechanotransduction: From tension to function. *Frontiers in Physiology* vol. 9 Preprint at https://doi.org/10.3389/fphys.2018.00824 (2018).
49. Zhu, C., Bao, G. & Wang, N. Cell Mechanics: Mechanical Response, Cell Adhesion, and Molecular Deformation. *Annu Rev Biomed Eng* (2000).
50. Tarbell, J. M., Simon, S. I. & Curry, F. R. E. Mechanosensing at the vascular interface. *Annual Review of Biomedical Engineering* vol. 16 505–532 Preprint at https://doi.org/10.1146/annurev-bioeng-071813-104908 (2014).
51. Wang, N. Review of Cellular Mechanotransduction Force-dependent integrin adhesion at cell-matrix interface. *Semin Cell Dev Biol* (2017).
52. Chen, C. S. Mechanotransduction - A field pulling together? *J Cell Sci* **121**, 3285–3292 (2008).
53. Huse, M. Mechanical forces in the immune system. *Nat Rev Immunol* **17**, 679–690 (2017).
54. Vestweber, D. How leukocytes cross the vascular endothelium. *Nature Reviews Immunology* vol. 15 692–704 Preprint at https://doi.org/10.1038/nri3908 (2015).
55. Salvermoser, M., Begandt, D., Alon, R. & Walzog, B. Nuclear deformation during neutrophil migration at sites of inflammation. *Frontiers in Immunology* vol. 9 Preprint at https://doi.org/10.3389/fimmu.2018.02680 (2018).
56. Schmid-Schönbein, G. W., Sung, K. L., Tözeren, H., Skalak, R. & Chien, S. Passive mechanical properties of human leukocytes. *Biophys J* **36**, 243–256 (1981).
57. Varshney, P., Yadav, V. & Saini, N. Lipid rafts in immune signalling: current progress and future perspective. *Immunology* vol. 149 13–24 Preprint at https://doi.org/10.1111/imm.12617 (2016).
58. Staubach, S. & Hanisch, F. G. Lipid rafts: Signaling and sorting platforms of cells and their roles in cancer. *Expert Review of Proteomics* vol. 8 263–277 Preprint at https://doi.org/10.1586/epr.11.2 (2011).
59. Montresor, A. *et al.* CXCR4-and BCR-triggered integrin activation in B-cell chronic lymphocytic leukemia cells depends on JAK2-activated Bruton's tyrosine kinase. *Oncotarget* (2018).
60. Devreotes, P. & Horwitz, A. R. Signaling Networks that Regulate Cell Migration. *Cold Spring Harb Perspect Biol* (2015) doi:10.1101/cshperspect.a005959.

61. Salvermoser, M., Begandt, D., Alon, R. & Walzog, B. Nuclear deformation during neutrophil migration at sites of inflammation. *Frontiers in Immunology* vol. 9 Preprint at https://doi.org/10.3389/fimmu.2018.02680 (2018).
62. Kameritsch, P. & Renkawitz, J. Principles of Leukocyte Migration Strategies. *Trends in Cell Biology* vol. 30 818–832 Preprint at https://doi.org/10.1016/j.tcb.2020.06.007 (2020).
63. Graham, D. M. *et al.* Enucleated cells reveal differential roles of the nucleus in cell migration, polarity, and mechanotransduction. *Journal of Cell Biology* **217**, 895–914 (2018).
64. von Andrian, U. H., Hasslen, S. R., Nelson, R. D., Erlandsen, S. L. & Butchert, E. C. *A Central Role for Microvillous Receptor Presentation in Leukocyte Adhesion under Flow*. *Cell* vol. 82 (1995).
65. Kulke, M. *et al.* Interaction Between PEVK-Titin and Actin Filaments. *Circ Res* **89**, 874–881 (2001).
66. Cebecauer, M. Role of Lipids in Morphogenesis of T-Cell Microvilli. *Front Immunol* **12**, (2021).
67. Yi, J. C. & Samelson, L. E. Microvilli set the stage for T-cell activation. *Proc Natl Acad Sci U S A* **113**, 11061–11062 (2016).
68. Donnaloja, F., Carnevali, F., Jacchetti, E. & Raimondi, M. T. Lamin A/C Mechanotransduction in Laminopathies. *Cells* vol. 9 Preprint at https://doi.org/10.3390/cells9051306 (2020).
69. Makarov, A. A. *et al.* Lamin A molecular compression and sliding as mechanisms behind nucleoskeleton elasticity. *Nat Commun* **10**, (2019).
70. Hamouda, M. S., Labouesse, C. & Chalut, K. J. Nuclear mechanotransduction in stem cells. *Current opinion in cell biology* vol. 64 97–104 Preprint at https://doi.org/10.1016/j.ceb.2020.05.005 (2020).
71. Patteson, A. E. *et al.* Vimentin protects cells against nuclear rupture and DNA damage during migration. *Journal of Cell Biology* **218**, 4079–4092 (2019).
72. Brown, M. J., Hallam, J. A., Colucci-Guyon, E. & Shaw, S. *Rigidity of Circulating Lymphocytes Is Primarily Conferred by Vimentin Intermediate Filaments*. *The Journal of Immunology* vol. 166 (2001).
73. Machado, C. & Andrew, D. J. D-Titin: A giant protein with dual roles in chromosomes and muscles. *Journal of Cell Biology* **151**, 639–651 (2000).

74. Zastrow, M. S., Flaherty, D. B., Benian, G. M. & Wilson, K. L. Nuclear titin interacts with A- and B-type lamins in vitro and in vivo. *J Cell Sci* **119**, 239–249 (2006).
75. Hashimoto, K. *et al.* Nuclear connectin novex-3 promotes proliferation of hypoxic foetal cardiomyocytes. *Sci Rep* **8**, (2018).
76. Giammarco, S. *et al.* Hyperleukocytosis and leukostasis: management of a medical emergency. *Expert Rev Hematol* **10**, 147–154 (2017).
77. Rosenbluth, M. J., Lam, W. A. & Fletcher, D. A. Force microscopy of nonadherent cells: A comparison of leukemia cell deformability. *Biophys J* **90**, 2994–3003 (2006).
78. Preira, P. *et al.* The leukocyte-stiffening property of plasma in early acute respiratory distress syndrome (ARDS) revealed by a microfluidic single-cell study: The role of cytokines and protection with antibodies. *Crit Care* **20**, (2016).
79. Neiva-Sousa, M., Almeida-Coelho, J., Falcão-Pires, I. & Leite-Moreira, A. F. Titin mutations: the fall of Goliath. *Heart Fail Rev* **20**, 579–588 (2015).